# CHALMERS

Space for picture

.

The report is intended to be printed double-sided.

# Development of an advanced three dimensional dummy neck

ODD Neck II

## DIEGO ASTUY GONZÁLEZ

Crash Safety Division

*Department of Machine and Vehicle Systems*          Master's Thesis June 2004

CHALMERS UNIVERSITY OF TECHNOLOGY

Göteborg, Sweden 2004

# Development of an advanced three dimensional dummy neck

## ODD Neck II

**DIEGO ASTUY GONZÁLEZ**

*In loving memory of Paca, Cari  y Luciano*

# ABSTRACT

Neck injuries in car accidents have become a serious problem over the last years. The most common neck injuries are often referred to as whiplash associated disorders due to the movement of the neck produced, although they have a low threat to life they are a major concern for the modern society in terms of both injury and cost. During recent years new techniques and methods for reducing whiplash injuries in the automotive field have been introduced. However, they have some limitation: they just focus on rear-end impact and does not take into account the other impact modes in which whiplash injuries occur. Further investigations done have showed that other impacts such as frontal or frontal oblique may be as large a problem as rear-end impact is. Due to the relationship established between the rear-end collision and the whiplash investigation most developed dummies designs were only able to perform flexion-extension motion but it is important to consider the lateral movements involved in most car accidents

The objective of this research was to design and manufacture a new omni directional dummy neck with the same three dimensional range of motion in each vertebra joint as human neck has.

The new prototype manufactured in this work, which is based on BioRID II, represents the skeletal cervical spine and all its movements in any direction. Not only does it replicate the movement pattern, furthermore, it has a biofidelic performance that closely simulates the behaviour of the human neck in both range of motion and stiffness. It would be feasible to use it on any kind of car impacts: lateral, oblique, roll-over, far side, frontal and rear-end impacts

Although aspects like dynamic properties, durability and repeatability were not studied in this thesis, the prototype represents a good basis for further studies in multidirectional dummy necks that will contribute to a better understanding of neck injury mechanisms.


*Keywords*: omni-directional, dummy, neck, lateral bending, axial rotation, coupled movement, whiplash, BioRID, prototype, range of motion, stiffness.

# ACKNOWLEDGEMENTS

# CONTENTS

# 1. INTRODUCTION

Neck injuries in car accidents have become a serious problem over the last years. These injuries are responsible for one third of all automotive injuries leading to permanent disability [21]. Most neck injuries, however, are minor injuries with a low threat to life. These injuries are often referred to as whiplash associated disorders (WAD). Although classified as minor injuries, they can have serious consequences for the patient's professional and personal life, due to the often long-lasting symptoms. The comparison of major accident samples from the German Motor insurers shows that the incidence of WAD in Motor Vehicle Accidents has almost doubled in the last 20 years [15]. Whiplash injury due to car collisions is one of the most aggravating traffic safety problems with serious implications for the European society. Yearly more than a million European citizens suffer neck injuries implying tremendous societal cost (roughly at least 10 Billion Euro [30]). WAD are a major concern for the modern society in terms of both injury and cost. A lot of work should be taken in trying to quantify the problem and determine means of injury and cost reduction.

In order to predict the behaviour of the human body during impact in car accidents several methods are used. Crash test with dummies, volunteers, Post Mortem Human Subjects (PMHS) and mathematical models are different ways to approach the problem. Data taken from PMHS and volunteer test are applied to validate crash test dummies and mathematical models. Crash test dummies should have a human-like performance with repeated and reproductive features.

## 1.1 PROBLEM FORMULATION

During recent years new techniques and methods for reducing WAD in the automotive field have been introduced. Many of these developments focus on rear-end impact only and do not take into account the other impact modes in which whiplash injuries occur. Further investigations [3] done have showed that frontal impact may be as large a problem as rear-end impact is, even though injury risks are lower. Inside the frontal accidents with WAD, the frontal oblique collisions show the highest incidence of injury (60-70% of the frontal accidents are offset [10]) and the impact severity in frontal accidents is significantly higher than in rear-end accidents.

Due to the relationship established between the rear-end collision and the whiplash investigation most dummies designs developed were only able to perform flexion-extension motion but it is important to consider the lateral movements involved in most of car accidents.

## 1.2 OBJECTIVE

The objective of this research is to design and manufacture a new omni directional dummy neck. The work carried out with this thesis is meant to continue and improve the development of a previous Omni-Directional Dummy neck prototype (ODD neck) [4]. It should replicate with a humanlike behaviour the four main movements and

stiffness properties of the human neck in order to make the dummy feasible to use it on any kind of impacts: lateral, oblique, roll-over, far side, frontal and rear-end. Then, the prototype will contribute to a better understanding of injury mechanisms.

## 1.3 BIOMECHANICS OF THE HUMAN CERVICAL SPINE

### 1.3.1 Functional Anatomy of the spine

This section reviews the essential parts of the human spine. The cervical spine comprises seven bony elements, called vertebrae, which are joined by soft tissues. Within these tissues are the intervertebral discs, the muscles and the ligaments.

**Vertebrae.** The cervical spine has seven vertebrae, referred as C1 to C7 from the top, which constitute the neck. (Fig. 1-1) The main roles of this upper spine segment are to hold the head up, allow its different movements and protect the spinal cord. Among these seven vertebrae, the first and second vertebrae, atlas and axis, are distinct from each other and from the lower five vertebrae, which are similar in shape and functionality.
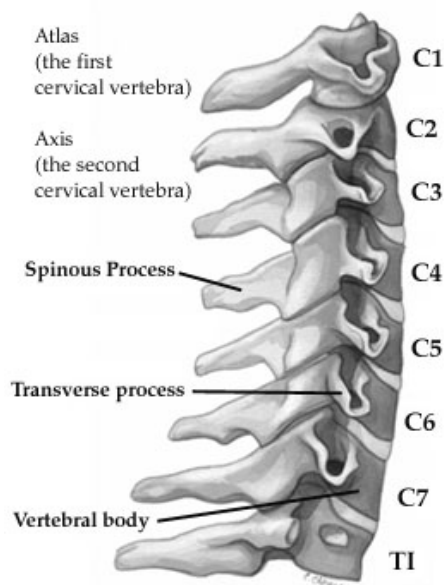


**Fig. 1-1** Neck structure (adapted from Hughston Sports Medicine Foundation)

Due to these differences, the cervical vertebral column can be divided into the lower and the upper cervical spine.

The upper cervical spine comprises axis, atlas and occiput, and is also called the occipito-atlanto axial region. The occiput (C0) is the base of the skull and articulates with the atlas. The atlas, C1, (Fig. 1-2) has no vertebral body, but consists of a bony ring with a pair of cartilaginous facets on its superior side which are cup shaped and let the occiput gliding on them to perform extension, flexion and lateral bending. The atlas vertebra foramen (the hole in the vertebra body) is remarkably larger compared to those in the rest of any other vertebrae. Besides the spinal cord, it must accommodate the dens of the axis through its anterior side.

2

# Vertebrae C1 The atlas



**Superior view**          **Oblique view**

**Fig. 1-2** Atlas (adapted from Human Anatomy&Physiology[5])

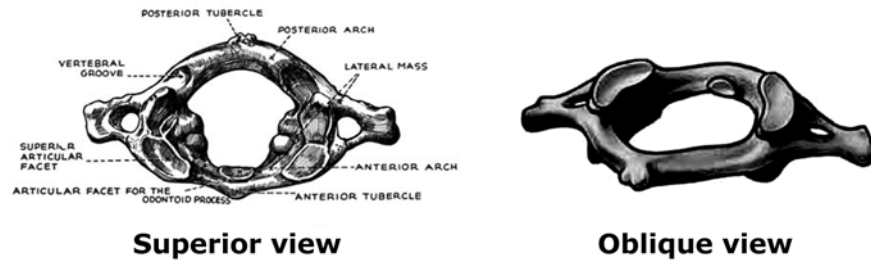The second cervical vertebra called the axis, C2, (Fig. 1-3) comprises a body and an arch, but it has an additional element, the odontoid process or dens, a blunt tooth-like process that project upwards from the vertebra body. It provides a type of pivot and collar allowing the head and the atlas to rotate around the dens.

# Vertebrae C2 The Axis



**Anterior view**          **Side view**
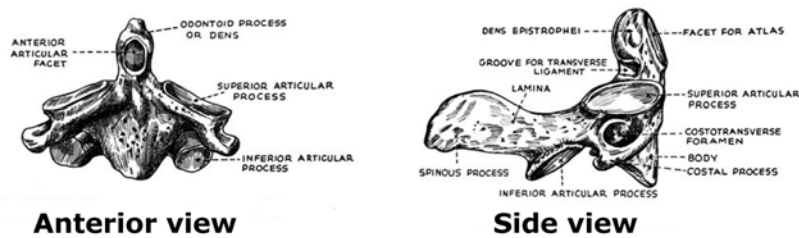
**Fig. 1-3** Axis (adapted from Human Anatomy&Physiology [5])

The lower cervical region consists of vertebrae C3 through C7 (Fig. 1-4&1-5), each of which comprises of a cylindrically shaped body and an arch. These enclose the vertebral foramen which forms the spinal canal through which the spinal cord passes. The arch includes two pairs of articular facets, a spinous process and two transverse processes. The processes constitute attachment points for muscles and ligaments. The posterior spinous process will come in contact when the neck performs hyperextension, extreme movement in extension, and the transverse processes will behave closely on lateral bending.

# Vertebrae C3



**Superior view**          **Frontal view**

**Fig. 1-4** C3 (adapted from Human Anatomy&Physiology [5])

The articular facets are almost flat, covered with cartilage and obliquely oriented with different values of angles (Fig. 1-5) from one vertebra to another but with a mean backward angle of about 42 degrees in the sagittal plane.

# Vertebrae C3   Lower cervical



**Side view**          **Facets orientation**

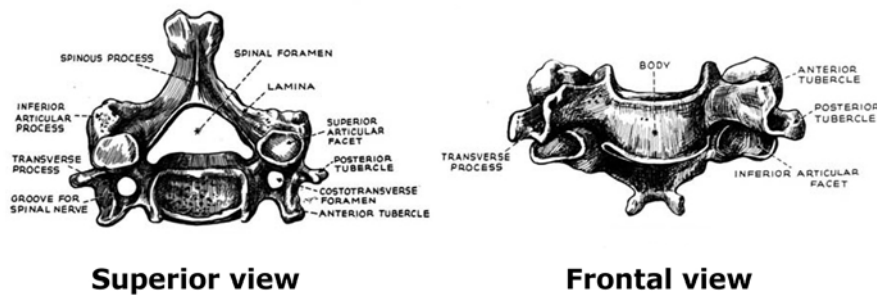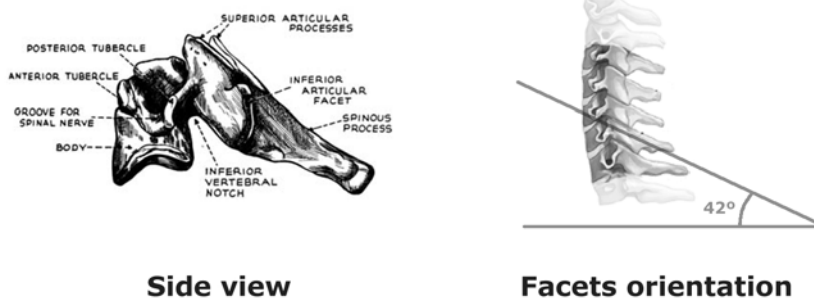**Fig. 1-5** C3 side view and lower spine facets orientation (adapted from Human Anatomy&Physiology [5])

**Intervertebral discs.** They are placed between two adjacent vertebrae except concerning the occipito-atlanto-axial region. The discs are a fibrocartilaginous joints that allow movement in all directions and work as a damper. They are thicker anterior than posterior and provide the cervical spine an anteriorly convex curve, called cervical lordosis. Due to their composition, the discs are more sensitive to rotational strain than to compression, tension and shear.

**Ligaments.** The spinal cord is protected from excessive motion by the ligaments. They also allow spinal motion within physiologic range. There are both short ligaments that connect adjacent vertebrae, like the transverse ligament, and longer ones that extend over several vertebrae such as the longitudinal anterior and posterior ligament. The anterior longitudinal ligament limits the extension of the spine while the posterior ligaments limit the flexion. The transverse ligament placed in the atlas holds the dens against the anterior arch of the atlas to constrain the dens subsequently.

**Muscles**. They are needed to maintain the head and neck stability and to produce movements of the head and neck. Due to the midsagittal symmetry, muscles appear twice, on every side of the cervical spine. Although the muscular system of the spine is very complex, it can be divided into three groups: deep muscles which attached two adjacent vertebrae controlling their movements, intermediate muscles that run from

cervical vertebrae to the thorax or connect the spine with the skull with different links and, finally, superficial muscles which bond without attachments to the vertebrae from the head to the thoracic region..

## 1.3.2 Kinematics of the neck

The cervical spine has free mobility in a multitude of directions but it can be described in four main movements (Fig. 1-6), although it is rather usual to find any combination (coupling) of those.
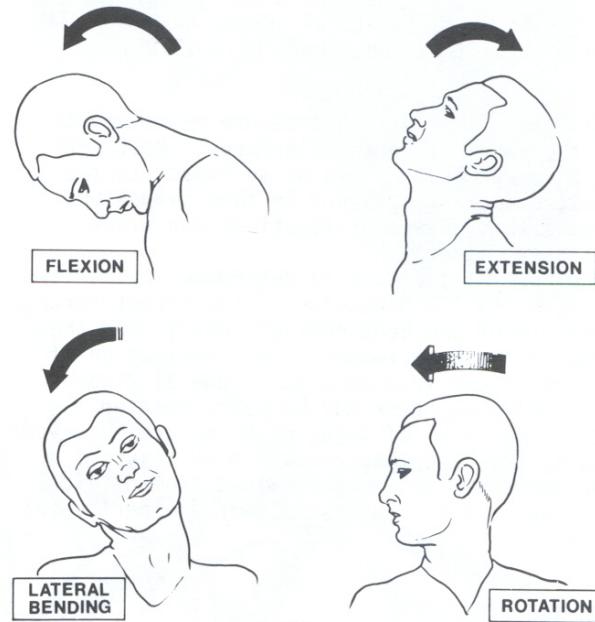


**Fig. 1-6** Main displacements of the neck (adapted from Huelke[17])

Bending forward placing the face toward the chest is flexion, bending backwards, extension. Laying the head right or left by putting the ear toward the shoulder is lateral bending and turning the head from side to side is rotation.

The movement of the head is controlled by the overall movements of each of the cervical vertebrae added together. However, certain vertebrae have unique types and range of motion. The atlas allows slight forward and a larger backward head nodding due to its joint with the occiput. The joint between axis and C2 lets slight rotation of the head relative to the neck. The lower cervical spine has a particular behaviour coupled movement, replicated mechanically in the designed dummy, due to the spatial orientation of the facet joints. Axial rotation is associated with lateral bending such the spinous processes move to the left when the head and neck are bent to right (Fig.1-7). Even though this coupled movement always takes place in the lower cervical spine, the head is able to turn horizontally balanced by the particular shape and performance of the upper spine.
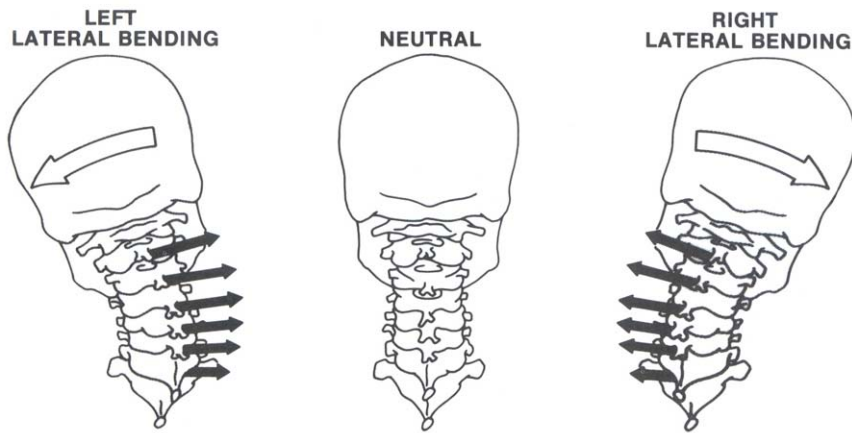
**Fig. 1-7** Spine orientation due to lateral bending (adapted from Panjabi[31])

rvertebral disc?

### 1.3.3 Range of Motion

The difference between the two points of physiologic extremes of movement is the range of motion (ROM). In the cervical spine, measured in the four main directions, these two points are considered from the rest position of the neck to its maximum allowed position on each movement.

The value of ROM varies from individual to individual depending on several factors such as age, gender and person's elasticity.

Several studies have been carried out in the last years to determine the ROM using different techniques.

**Table 1** Range of Motion (degrees) of the cervical spine

| Author | Motion | C0C1 | C1C2 | C2C3 | C3C4 | C4C5 | C5C6 | C7C8 | Total |
|--------|--------|------|------|------|------|------|------|------|-------|
| White and Panjabi [16] | Combined F/E | 25 | 20 | 10 | 15 | 20 | 20 | 17 | 127 |
| | One Side L.B. | 5 | 5 | 10 | 11 | 11 | 8 | 7 | 114 |
| | One Side A.R. | 5 | 40 | 3 | 7 | 7 | 7 | 6 | 150 |
| Kapandji [10] | Combined F/E | 20-30 | | 100-110 | | | | | 130 |
| | One Side L.B. | 8 | | 45 | | | | | 106 |
| | One Side A.R. | 12 | | 68-78 | | | | | 160-180 |
| Feipel [11] | Combined F/E | | | | | | | | 122 |
| | Total L.B. | | | | | | | | 88 |
| | Total A.R. | | | | | | | | 144 |
| Mannion [12] | Combined F/E | | | | | | | | 129.3 |
| | Total L.B | | | | | | | | 85.1 |
| | Total A.R.. | | | | | | | | 151.3 |
| LoPresti [13] | Combined F/E | | | | | | | | 118.4 |
| | Total L.B. | | | | | | | | 87.4 |
| | Total A.R.. | | | | | | | | 137.9 |

The first approach used radiographs to measure the angle of in-vivo and in-vitro subjects [31, 18], which provide the most suitable values of ROM between adjacent vertebrae. But there are other methods that have been applied to find out the ROM of the spine like the anatomical studies, electrogoniometric devices [9, 22] and computer based tools using ultrasonic transmitter [20]. These latter ones present values for global ROM of the neck that can be used to validate the global neck dummy.

### 1.3.4 Mechanical Characteristics

Mechanical characteristics of biological tissues are necessary in determining the dummy design properties. These properties vary on every individual as it happens with the ROM depending on same factor such as age, gender, etc. The stiffness attributes of the neck in main movements should be considered to get a reliable dummy. Motion segments or ligaments like neck ones typically have a nonlinear, sigmoidal shape load-displacement curve [8].
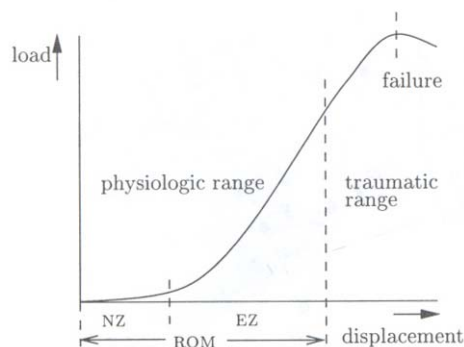


**Fig. 1-8** Typical Load-Displacement curve for biomechanical structures (adapted from de Jager[8])

The curve (Fig. 1-8) shows two areas: the physiologic range of motion that characterizes the amount of displacement that the motion segment is able to sustain without being damaged and the traumatic range. The former zone in turn has two areas, the neutral zone in which little load is needed to deform the structure and the elastic, where the load is considerable increased but the specimen will return to the state it had before when the load is released. The design dummy will replicate this particular human behaviour thanks to the use of some rubber cushions between adjacent vertebrae.

Stiffness and flexibility are used to describe the load-displacement curves. Stiffness is defined as the ratio of the load applied to the displacement produced. Flexibility is the reciprocal of stiffness. Due to the nonlinear behaviour of the curve the stiffness varies along it, therefore different methods were developed to estimate this slope, so the range of load and displacement for which the stiffness were calculated should be given.

re?

## 1.4 EXISTING DUMMIES

Several crash test dummies have been developed in the last years in order to replicate the human behaviour and improve the safety in the automotive field. Depending on the sort of impacts to study, different characteristic are implemented in the dummy. A brief description of the available dummies designed is carried out next.

## 1.4.1 Hybrid III

Hybrid III is the standard dummy used in frontal crash tests all over the world. It was developed for General Motors. The Hybrid III dummy neck (Fig. 1-9) has three rigid aluminium discs separate a flexible component made of butyl elastomer.



**Fig. 1-9** Hybrid III 50th percentile Head&Neck (adapted from Denton Atd, Inc.)

There are a range of Hybrid III dummies depending on the population that represent; the most widely used is 50th percentile which represents an average size and weight of the men population. A lack of biofidelity in the stiffness of this dummy in the frontal impacts has been discovered [29], advising against its use in particular situations and suggesting new developments.

## 1.4.2 SID, BIOSID, EUROSID, WORLDSID

They were designed for a deep study of lateral impacts. The SID was the first attempt to study the side impacts developed by National Highway Traffic Safety Administration (NHTSA). BioSID is based on the Hybrid III neck so it doesn't have any relevant modifications in the neck.

EuroSID (Fig. 1-10) has been created by European Experimental Vehicles Committee (EECV).There are two versions of this dummy called EuroSID 1 and EuroSID 2. Both of them have a neck made by a composition of metal discs and rubber elements with special joints to head and chest to allow a realistic motion of the head relative to the chest.
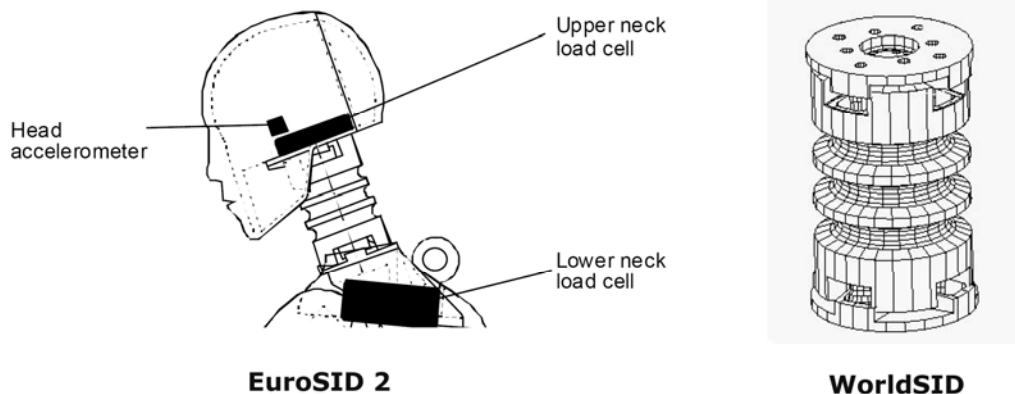


**Fig. 1-10** Neck schematics from EuroSID and WorldSID(adapted from EEVC and ISO respectively)

Recently, International Standard Organization (ISO) has completed the development of the WorldSID dummy (Fig. 1-10) with the cooperation from several countries in the world, including Europe and USA joining their efforts. The neck of the WorldSID has a central deformable element, bracket to adjust pre-impact orientation and a shroud to avoid unrealistic interactions.

All the dummies described previously are designed to represent 50th percentile of average-size men

### 1.4.3 Thor

This 50th percentile male dummy was developed by National Highway Traffic Safety Administration (NHTSA),

The neck (Fig. 1-11) is made from a series of aluminium discs and rubber pucks which are bonded together and also has compression springs attached to simulate the effects of the musculature.
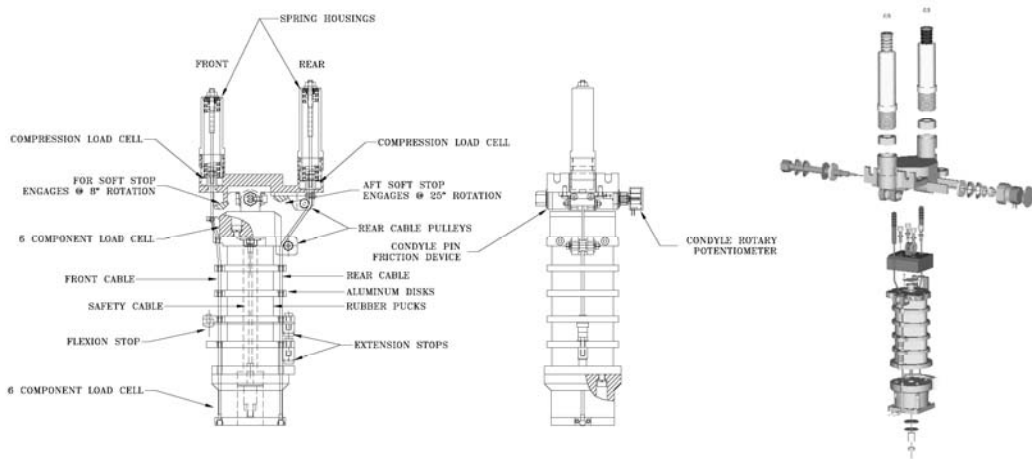


**Fig. 1-11** Thor neck (adapted from NHTSA)

Although it was devised for frontal impacts due to the multi-directional head/neck system, it would provide good results in lateral and oblique tests.

### 1.4.4 BioRID II

The BioRID-II was developed as a 50th percentile male dummy to measure responses in low speed rear-end impact tests. BioRID's neck (Fig. 1-12) is composed of seven vertebra-like pieces, so that in a rear-end crash interacts in a more humanlike way than any other dummy.
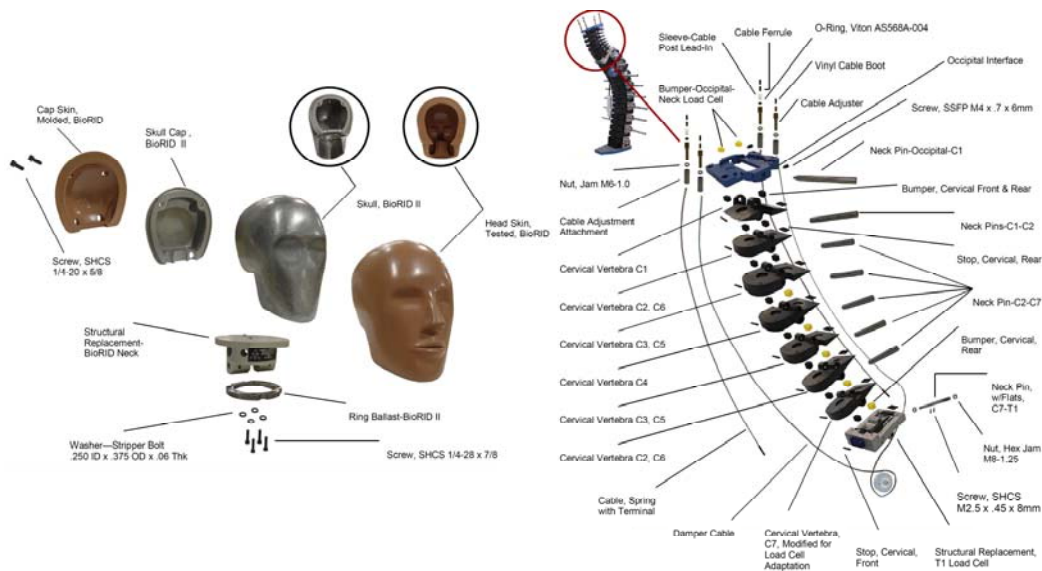
**Fig. 1-12** BioRID II Head&Neck (adapted from Denton Atd, Inc.)

Each vertebra is made of composite material and connected to each other by pin joints to allow angular motion only in sagittal plane; therefore this dummy can just perform flexion and extension. The motion of the cervical vertebrae assembly is controlled by a single cable attached to a damper and two cables attached to springs that act as neck-muscle substitutes. Also included between the vertebrae are elastomer bumpers to control the end of travel response.

er dummies?

# 2. ODD-ɴᴇᴄᴋ II: Sᴋᴇʟᴇᴛᴀʟ Bᴏᴅʏ

The objective of this chapter is to present the basic components of the dummy: vertebrae and joints. The dummy neck is based on a previous propose, ODD neck [4], which is inspired in turn by BioRID. This neck stands out because of its resemblance to the human body. It comprises (Fig. 2-1) seven vertebrae and one occiput interface. All vertebrae are identical but the C1, detailed drawings of each piece are presented on the Appendix.
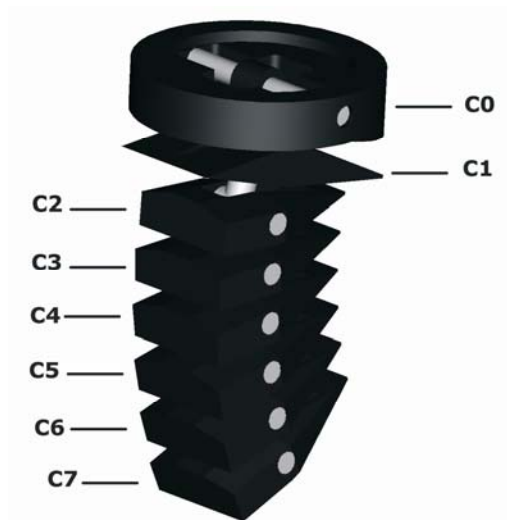


**Fig 2-1** General 3D model of the skeletal part of the neck with all the vertebrae and joints

## 2.1 Uᴘᴘᴇʀ ᴄᴇʀᴠɪᴄᴀʟ

Because of the fact that the neck pretends to imitate the human behaviour, its design can be split like the human neck does in upper cervical and lower cervical. The upper cervical of the prototype consists of three vertebrae: an occiput interface (C0), C1 and C2 and several joints solution to connect them. The neck attaches to the head by means of the C0 (Fig. 2-2) that has been completely redefined from the earlier version (ODD neck I).



**Fig. 2-2** Occiput interface, C0, views: manufacture prototype, 3D model, wireframe.

It has a circular shape with an inside hole across it to fit the BioRID head through its neck load cell modification. A horizontal pin joint is used to link the C0 to the head. A thin plastic layer is placed between C0 and the head interface to avoid movements from the occiput and fix its position.

The C1 vertebra (Fig. 2-3) has a particular profile rather different than any other vertebra to allow the dummy to replicate the particular behaviour of the upper cervical spine.



**Fig. 2-3** C1 views: manufacture prototype, 3D model, wireframe

It has an underneath threaded hole to fasten perpendicularly to C2 while the upper part consists of two jutting out parts, which are round off in the top to let the piece rotate around the joint. A horizontal hole goes across this underneath parts to allow the connection with C0. C2 presents the same design that the rest of the vertebrae which set up the lower neck so it will be described later.

The vertebrae were devised to imitate human body therefore the development of the joint solutions between vertebrae was done on its basis.
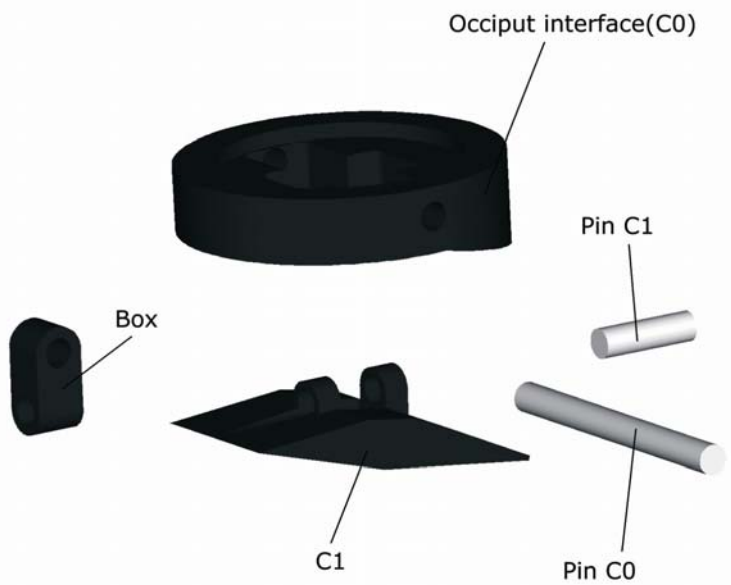


**Fig 2-4** Joint system between C0C1

The mechanical joint solution between occiput and C1 (Fig. 2-4) is a box with two pin-joints. It has round sides next to the pins to allow the rotation of the box across them.

Each of the pin joints permits one movement (Fig.2-5), flexion and extension in the upper joint and lateral bending in the lower one. The box is placed without an angle related, so pure moments are obtained in both directions. Based on review of literature [31], axial rotation was neglected between these vertebrae to simplify the design.
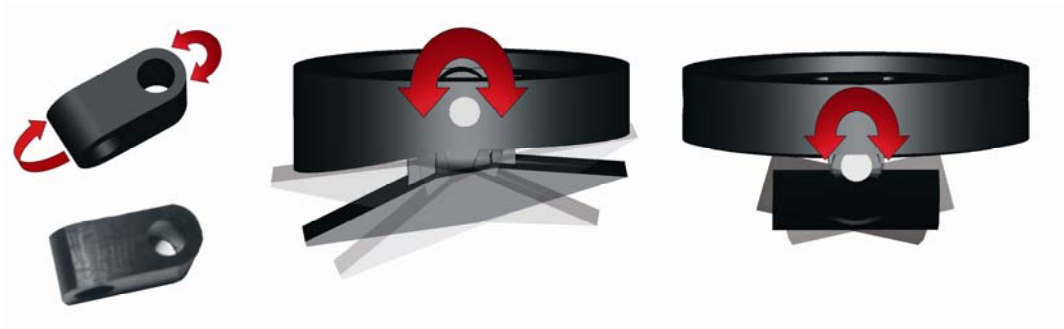
**Fig. 2-5** Box views: 3D model, manufacture prototype and possible movements between C0C1: flexion/extension and lateral bending

The joint between C1 and C2 (Fig. 2-6) shares design with the ones used in the lower cervical except for the size.
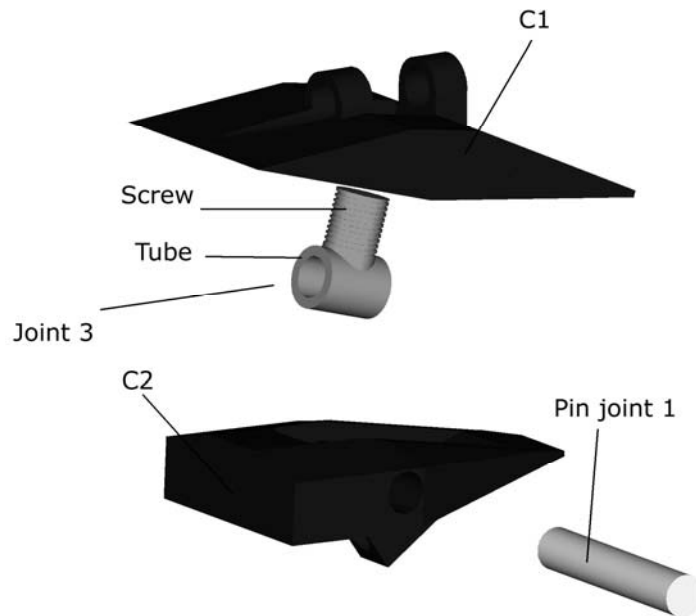


**Fig 2-6** Joint solutions between C1 and C2

It is made of two main parts, a tube part which together with a pin connect the vertebra to C2 allowing flexion/extension and a thread weld to the tube that screws down to the C1.



**Fig. 2-7** C1-C2.Posible movements between them: axial rotation and flexion/extension

Its special feature (Fig. 2-7) is that lateral bending is avoided by fastening C1 in a vertical position; then just flexion, extension and pure axial rotation are possible between vertebrae. Lateral bending was neglected in this joint [31] to make it simpler within a reasonable humanlike behaviour.

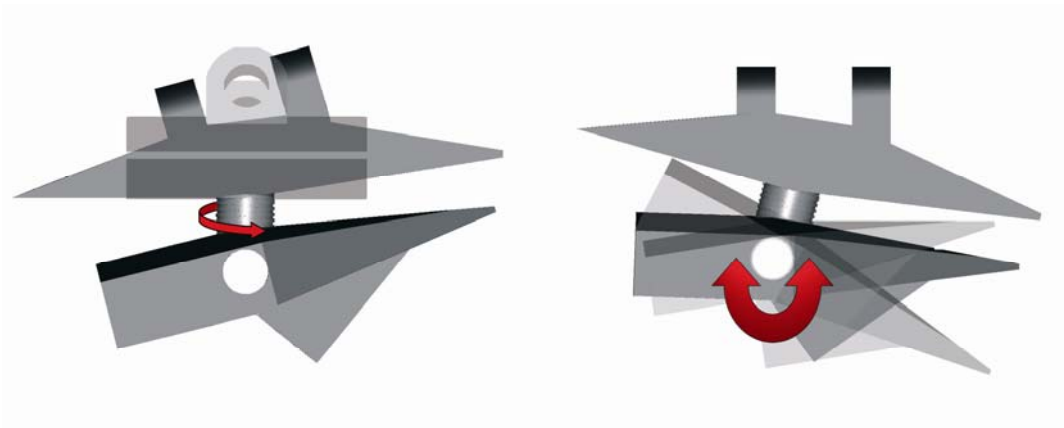## 2.2 LOWER CERVICAL

The lower cervical comprises vertebrae from C3 to C7 and unlike the human body, where they have different size, they are identical in the dummy (Fig. 2-8). It is based on BioRID but it has slope sides to enable the lateral bending/axial rotation and the centre of the vertebrae is adjusted to fit with the new joint system that will be discussed later.



**Fig. 2-8** Lower cervical vertebra views: manufacture prototype, 3D model, wireframe

Some modifications to the former version of the prototype were made, mainly round of some corner shapes to make the manufacture process easier.

The human cervical spine has a curvature of about 37º from C0 to C7 in the default position (see Neutral Position) so the vertebrae are placed in the neck with an average angle of 5.3º to each other. The jutting underneath part of the vertebrae makes up the attachment point for the joint with the lower vertebra. Since this mechanical solution intends to simulate the articular processes which has an average of 42º in humans, the underneath part of the vertebra is located at an angle of 37º to compensate the former described angle between vertebrae in neutral position.

The main feature of the lower cervical spine is the coupled movement produced between lateral bending and axial rotation. This is fairly achieved thanks to the joint solution (Fig. 2-9) previously explained in the upper cervical.

14
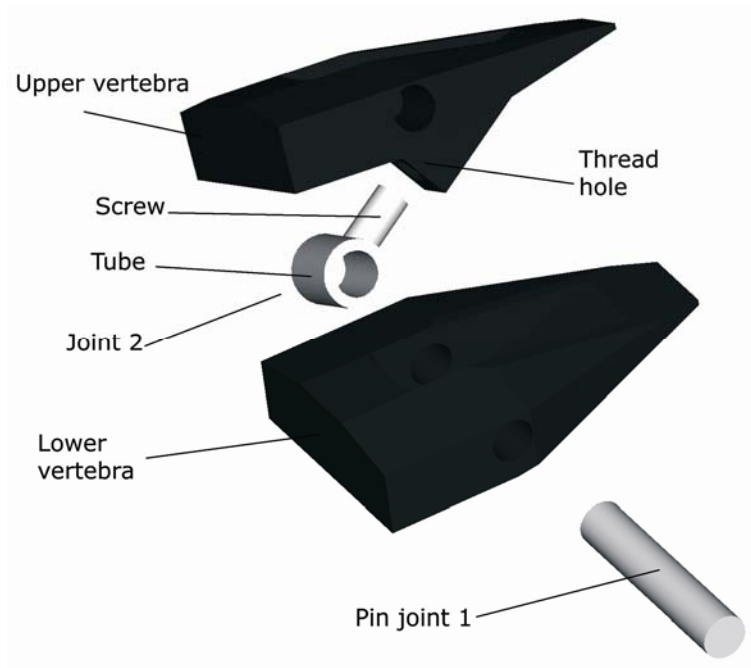
**Fig 2-9** Joint solutions designed between vertebrae in the lower cervical part of the dummy

The screw threaded part of the joint will substitute the articular processes providing guidance for flexion/extension and hindering lateral movement.
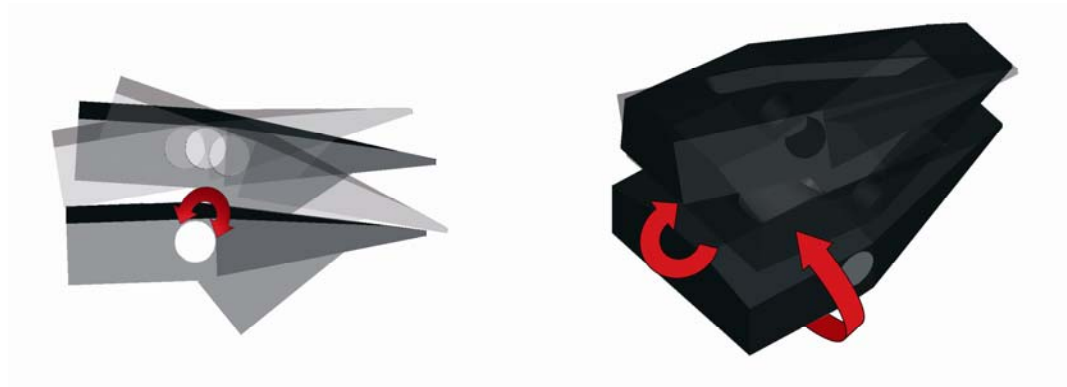


**Fig. 2-10** C3-C4. Possible movements: flexion/extension and couple lateral bending/axial rotation

Due to the connection between the tube and the screw, the rotation around the tube of the joint allows flexion/extension between vertebrae in the lower neck. The upper vertebra is screwed down to the joint and rotates around it. Due to the angle, which represents the average slope of the articular processes in the neck, a coupled movement of lateral bending and rotation similar to human body is created.

## 2.3 NEUTRAL POSITION

The initial position was defined [19] from the posture containing a lordosis and identified from the curvature of the neck (Fig.2-11) of a seated specimen.

**Fig 2-11** Default cervical spine curvature

The neck curvature follows the same curvature as the BioRID cervical spine. At this default position all the cervical joints centres are placed at an imaginary arch with a radius of 190mm and a sector of 37º. To achieve the neck spine curvature the intervertebral rubber bumpers fit in the space between vertebrae at their particular position.

## 2.4 RANGE OF MOTION

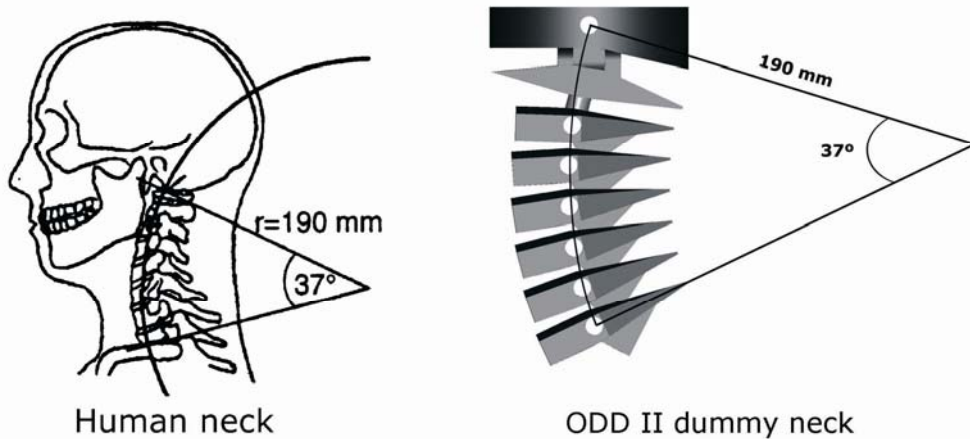The neck is designed to perform a range of motion (Table 2) within human values. Without any limitation place between vertebrae, the range of motion was designed based on in vivo studies [32] derived from examination of volunteers and including muscle effect of the neck. The movement is controlled by the shape of vertebrae and joints.

**Table 2** Range of motion of the prototype without any limitation between vertebrae and in-vivo values

| Motion | | C0C1 | C1C2 | C2C7[1] |
|---|---|---|---|---|
| Combined  F/E | In vivo[16] | 25 | 20 | 16.4 |
| | ODD-II | 27.8 | 37.1 | 27,5 |
| One Side L.B. | In vivo[16] | 5 | 5 | 9.4 |
| | ODD-II | 17 | - | 17.18[2] |
| One Side A.R. | In vivo[16] | 5 | 40 | 6 |
| | ODD-II | - | 180 | 10.74[b] |

Some assumptions have been made for simplicity and the range of motion is the same in the lower cervical for each vertebrae based on the mean value of the available data. The range of motion was increased a bit on every value for two reasons: on one hand to leave enough space between vertebrae to place rubber that may replicate stiffness properties of the neck; on the other hand to allow a movement a bit over the in

---

[1] Mean value from C2 to C7

[2] Calculate for the neutral position

16

vivo data because its values are based on volunteer test and the neck itself could go a bit further. It is important to point out that this dummy has not a size corresponding to a specific group of the population like the dummies showed before; the new prototype reproduces an average value of the whole population. The vertebrae were drawn with the aid of a computer three dimension CAD program and the range of motion was found out with the same software. After building the manufacture prototype, its range of motion was worked out with the aid of the TrackEye software to verify that the real values agree with the designed ones.

# 3. ODD-NECK II: INTERVERTEBRAL STIFFNESS PROPERTIES

## 3.1 INTRODUCTION

The mechanical behaviour of the human cervical spine is quantified by its physical properties. Among these properties, stiffness has an important role in mechanical characteristics of the complete cervical spine, motion segments and individual issues. The main achievement of this thesis was the development of a system that would be able to reproduce the stiffness properties of the neck. Since no reliable data were found to define in vivo properties between vertebrae, in vitro studies based on several test with cadavers were used to define the stiffness attributes. Although there are some quasi-static data available, just static studies were used to define the stiffness properties due to the complexity to set up a dynamic test procedure.

General observation from all referenced studies is that the variation in the data, quantified by the standard deviation is large. Standard deviation may be as large as 80% of the reported average stiffness or range of motion, and are seldom less than 10%. This reflects not only the large variability, which is typical for biological structures, but also limited accuracy and errors involved in these experiments, as they are extremely difficult to perform.

Because of the fact that in vitro values were taken, muscle reaction in the neck was not considered in the dummy. In a car collision at high speed (50km/h) the torques produced in the joints of the cervical spine by the external forces are much greater than those generated by the muscles. This means that the impact is closely correlated with the head-neck complex response. The reflex time the human body needs to activate the muscle might be long enough to keep the muscles relaxed. Hence the fact that the muscular effect is neglected, it wouldn't be a problem in high speed tests.

From all available options to get the stiffness neck properties, two mechanical solutions were developed to get the right one: place rubber cushions between the vertebrae, which compression will restrict the motion and cables to attach two vertebrae that will limit the range of motion by stretching it. Both of them have been used before in other dummies like BioRID verifying them as reliable alternatives.

### 3.1.1 Rubber

The first step in most product design is selecting the material to be used. Several factor such as function, shape and process should be taken into account of. Particularly in the neck, the key parameter to get the desire characteristic is the stiffness (spring) rate, the units are Newtons per meter (N/m). In terms of function, the stiffness rate of a part is defined as the amount of force required to cause a unit deflection:

$$K = \frac{F}{d} \quad \textbf{Eq.1}$$

Where $F$ is the applied force (N) and $d$ is the deflection (m), so the load-deflection characteristic would be linear. However, the target invertebral stiffness traces a nonlinear curve typical from biomechanic structures which has a hardening nonlinear behaviour. The rate of increasing deflection decelerates with increasing the force, thus the local stiffness is increasing with the increasing load. While in the neutral zone in the load-displacement curve of biomechanic components, the stiffness has a small value; it increases significantly in the elastic zone. Among all kind of materials, the most ordinary ones to show this behaviour are rubber components [27] under compression loads.

Due to the shape of the vertebrae and the placement of the rubber pieces between them, they are going to suffer compression and shear forces but the latter one are neglected because of the fact that they are relatively small compare with the former ones. The compression forces determine the range of motion between vertebrae.

### 3.1.2 Compression Stiffness: Theoretical

The compression stiffness rate of a rubber piece would be described as follow:

$$K_c = \frac{A \cdot E_c}{t} \quad \textbf{Eq.2}$$

where $A$ is effective load area ($m^2$), $t$ is thickness (m) of the undeformed polymer, and $E_c$ represents the compression moduli (kPa or $kN/m^2$) of the rubber. Compression moduli is strongly affected by the geometry of a design. values from this formulas are based on the principle that the operation remains in the linear range of the elastomer modulus, typically less than 30% strain for tension and compression which don't agree with the test, so this initial value is calculated as a based point and further test are developed to find the suitable material to be used.

Successful use of this equation depends on knowing the effective compression modulus $E_c$. The value of $E_c$ is a function of both material properties and component geometry. There are different methods to calculate the coefficient but an easy way [11] reasonably good in simple geometry, such as the ones applied in the design, is used to find out the effective $E_c$ value:

$$E_c = 1{,}33 \cdot E_0 \cdot \left(1 + \phi \cdot S^2\right) \quad \textbf{Eq.3}$$

The formulae describes the effective compression modulus for a flat sandwich block for one dimensional strain where $E_0$ is Young's modulus, $\phi$ is rubber compression coefficient and $S$ is shape factor. The coefficient $\phi$ is an empirically determined material property, which is included in the formulae to correct experimental deviation from theoretical equations. Several $\phi$ values related to other coefficients are shown:

**Table 3** Material properties (adapted from Gent[11])

| Shear modulus $G$ (kPa) | Young's modulus $E_0$ (kPa) | Bulk modulus $E_b$ (MPa) | Material compressibility coefficient, $\phi$ |
|---|---|---|---|
| 296 | 896 | 979 | 0.93 |
| 365 | 1158 | 979 | 0.89 |
| 441 | 1469 | 979 | 0.85 |
| 524 | 1765 | 979 | 0.80 |
| 621 | 2137 | 1007 | 0.73 |
| 793 | 3172 | 1062 | 0.64 |
| 1034 | 4344 | 1124 | 0.57 |
| 1344 | 5723 | 1179 | 0.54 |
| 1689 | 7170 | 1241 | 0.53 |
| 2186 | 9239 | 1303 | 0.52 |

The shape factor S is a component geometry function that describes geometric effects on the compression modulus. It is defined as the ratio of the area of one loaded surface to the total surface area that is free to bulge:

$$\text{shape factor } S = \frac{\text{load area}}{\text{bulge area}} = \frac{A_L}{A_B} \quad \textbf{Eq.4}$$

Rubber-like materials have unique deformation characteristics because their Poisson's ratio $\upsilon = 0.49 - 0.4995 \approx 0.5$. The modulus of volumetric compressibility is:

$$K = \frac{G}{(1 - 2 \cdot \upsilon)} \quad \textbf{Eq.5}$$

then it is approaching infinity when $\upsilon$ is closed to 0.5. Materials with $\upsilon = 0.5$ are not changing their volume under compression, thus rubber is practically a volumetric incompressible material. In some cases, bulk compressibility makes an appreciable contribution to the deformation of a thin rubber compression, and the apparent compression modulus approaches the bulk modulus in magnitude. Bearing in mind this decrease in stiffness rate, the calculated compression modulus should be multiplied by the following factor:

$$\frac{1}{1 + E_0 / E_b} \quad \textbf{Eq.6}$$

where $E_b$ is the modulus of bulk compression. Because of the fact that the loads applied to the rubber are not big enough in the performer test, this factor is neglected as it should be considered where large load are applied.

The elastic module of the rubber components is often characterized indirectly by measuring the elastic indentation caused by a rigid indentor of prescribed size and

shape, either a truncated cone or a sphere, pressed into the surface under specified loading conditions. Various nonlinear scales are employed to derive a value of rubber hardness from such measurements. One of these scales is Shore hardness which measures the resistance of a material to the penetration of a needle under a defined spring force. It is denoted as a number from 0 to 100 on the A. The higher the number, the higher the hardness. The A scale is the most widespread to define the softer types of rubber and the way of rubber's dealers identify their products commercially.

The depth of penetration of the indentor is directly related to the force required, thus durometer scale is typically used as a stiffness indicator (since both force and deflection are measured) [16]. Correlation values of Young's modulus $E$ and Shore A hardness scale are given:

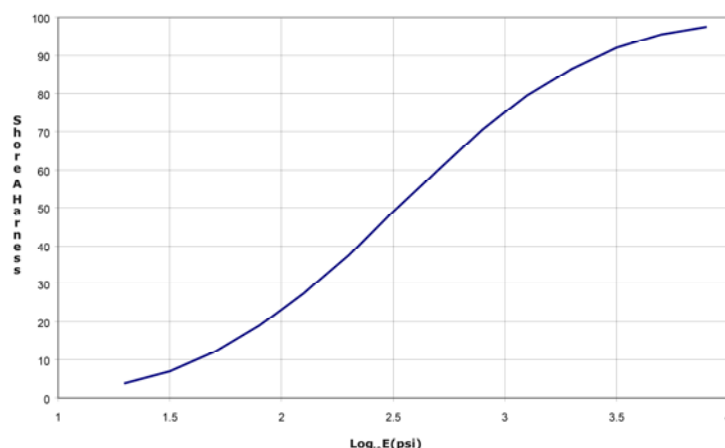| Hardness Shore A | 10 | 15 | 20 | 25 | 30 | 35 |
|---|---|---|---|---|---|---|
| Young's Modulus (MPa) | 0.27 | 0.43 | 0.57 | 0.77 | 1.14 | 1.44 |
| Hardness Shore A | 40 | 45 | 50 | 55 | 60 | 65 |
| Young's Modulus (MPa) | 1.,72 | 2.06 | 2.48 | 2.96 | 3.8 | 4.41 |
| Hardness Shore A | 70 | 75 | 80 | 85 | 90 | 95 |
| Young's Modulus (MPa) | 5.51 | 6.89 | 9.31 | 13.1 | 20.69 | 42.34 |



**Fig 3-1** Relation between indentation hardness and Young's modulus (adapted from Hertz[16])

With the aid of this conversion rates it is possible to find out theoretically the kind of rubber to be used between vertebrae to get the desired stiffness properties.

## 3.2 LOWER CERVICAL

A small number of studies computing the mechanical performance of segments of the lower cervical spine are available. Goel et al. [13, 12], Moroney et al. [23], Panjabi et al. [25,26] and Camacho et al.[2] measured static characteristic. All of them used a similar experimental set-up to test segments of the lower cervical spine: forces or moments were applied to the upper vertebrae while the lowest vertebra was firmly fixed to the test equipment. The main differences between studies are size of specimen (two vertebrae or more), number of them and application of loads. The range of applied loads differs from one study to another together with the axial preload that some of them applied to the vertebrae. Because of the fact that the neck was devised to fit the average values of the whole population and the vertebrae in the lower part of the dummy are identical, the average values of all studies were taken as pattern.

### 3.2.1 Flexion/Extension

From all available studies, Camacho et al. [2] was used to adjust the stiffness properties in flexion and extension on the lower cervical spine due to the detailed available data. Their study describes the static flexibility experiments on ten unembalmed male human head and cervical spine preparations. The sagittal plane bending responses were measured in a load frame designed to apply pure moments. Torques up to 1.5 Nm (flexion) and up to -1.5 Nm (extension) were applied in 0.1 Nm increments. For each motion segment the data points were fitted using the function:

$$\theta = \frac{1}{B} \cdot Ln\left(\frac{M}{A} + 1\right) \quad \textbf{Eq.7}$$

where A and B are constant coefficients for every vertebrae's couple, M is the applied moment and $\theta$ is the measured angular displacement.

### *3.2.1.1    Measurement instrument*

Some static tests were made to check that the model of the dummy neck fits to the values from the experimental studies. The sagittal plane bending responses of the vertebrae were tested by mean of a simple apparatus (Fig.3-2). It consists of an aluminium u-shape profile, a digital goniometer, a couple of magnetic pieces placed equidistantly from the centre, a screw and a drilled steel pin.
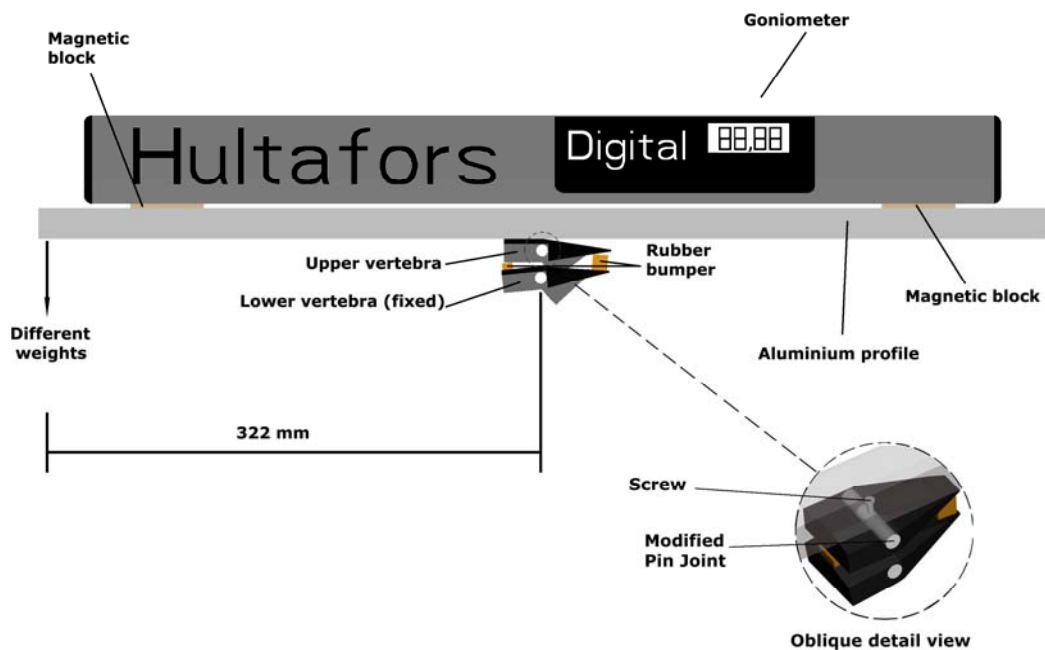


**Fig. 3-2** Sketch of the measuring instrument for flexion and extension in the lower cervical spine

The common pin joint between lower vertebrae is replaced by a modified pin joint with the same size but a thread hole is drilled in the middle. The aluminium bar is connected to the pin joint and to the lower vertebra by the screw and washer. The goniometer is fixed on the top of the aluminium by mean of the magnetic pieces. On one side of the profile another hole is drilled to a determined distance (322mm from the Rotation's centre in the lower vertebra). Hanging different weights it is possible to get the desired range of moments (0-1.5 N·m). Both extension and flexion tests have the

same procedure; they only differ on the position of the measuring instrument relative to the vertebrae

The lower vertebra is firmly clamped while the test apparatus is fitted to the upper vertebra then, by mean of changing the weights, different moments are applied to the lower vertebra and the displacement (angle) is displayed on the goniometer for each moment. There is a small deviation in the measurements (Fig.3-3) because of the angle itself and the vertical position of the applied force, so a correction with the cosine of the angle should be introduced.
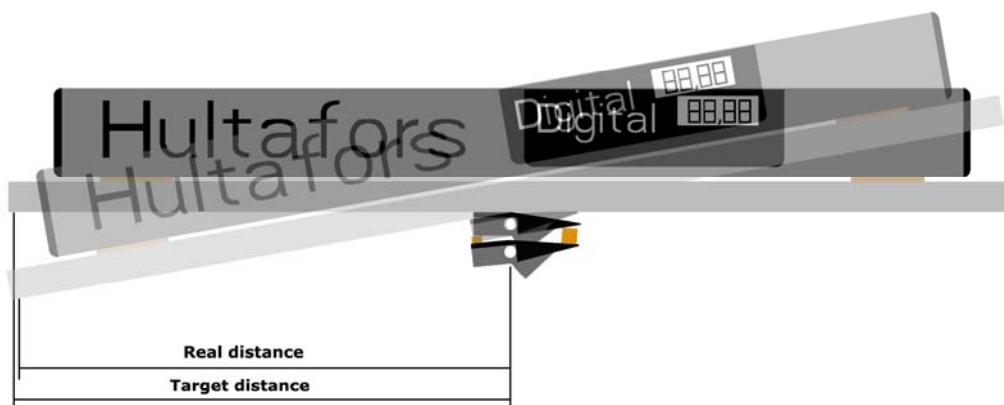


**Fig. 3-3** Deviation produced in the distance on every applied moment

The hanging weight creates a vertical load but the distance to the rotation's centre changes from the initial application of the weight to the final position that defines the relative displacement of the upper vertebra. This latter one was used to calculate the weight to produce the desired moment. Due to the decrease in the distance, a smaller moment than the target one is achieved. Although this deviation is quite small with lower angle such the one obtain in the lower cervical spin, it was corrected (it would be more important in the upper cervical as the angles are larger). The procedure to correct it was: first of all, perform a first test and record all the displacement's values for every moment, then these values were used to update the required weight to create every moment. The new weight's data are bigger than the first one because the real distance is smaller than 322mm, the one use to calculate the initial weights.

### 3.2.1.2    *First approach: Theoretical*

First of all, a prismatic shape of the rubber to place between vertebrae was chosen. The dimensions of the rubber fit perfect the intervertebral space (Table 4) in the neutral position of the neck and make them to hold this position.

**Table 4** Intervertebral space and rubber dimensions of the lower cervical spine (thickness on bold values)

|  | Intervertebral space | Rubber dimensions |
|---|---|---|
| Flexion | **4,35**x8,9x14 | **4,5**x8,9x14 |
| Extension | **9,82**x13,49x14 | **10**x13x14 |

The previous limitation together with the restriction of the vertebrae design to glue the rubber defines the rubber size. With the aid of the 3D model of the vertebra in CAD software dimensions were determined. The final size was increased a bit in its thickness, which control the range of motion, to get a bit of compression in the setting up and improve the stability of the model at the default position.

The average stiffness rate (Fig.3-4) value was computed from all cervical in the lower spine (C2-C7) based on available data because the dummy vertebrae in the lower part are identical in shape and range of motion unlike the human ones that have different size and motion each one.
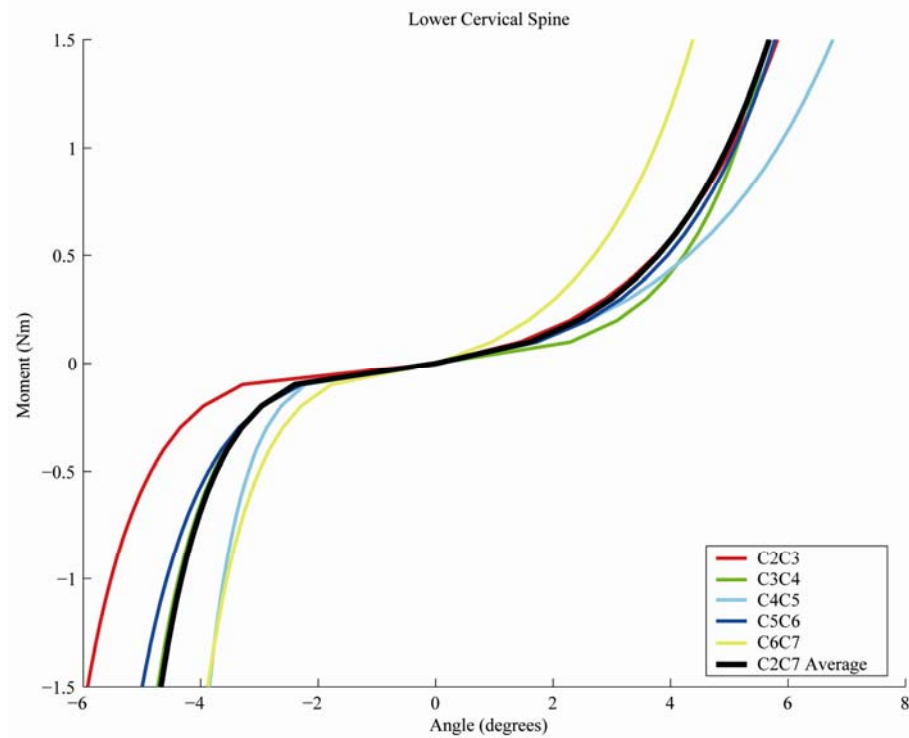


**Fig. 3-4** Load-displacement curves of the lower cervical spine from Camacho et al.

These stiffness values due to the inherent properties of the biomechanic structures are not constant but variables. Therefore the extreme values from the data were chosen arbitrarily to set up the first theoretical value of rubber to be tested. The average lower cervical displacement of Camacho et al. at ±1.5 N·m are respectively -4.677° and 5.6825° (positive for flexion and negative for extension).

It was worked out the final thickness in the 3D model that it would give the desired range of motion to calculate the deflection the rubber should have (Fig.3-5): 1.87mm at flexion and 2.88mm at extension.
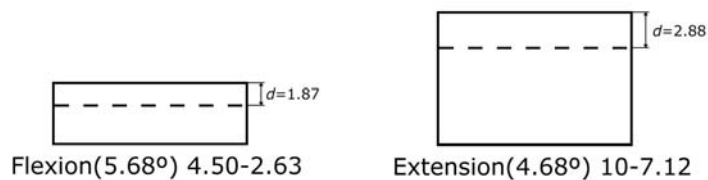


**Fig. 3-5** Rubber target deflection at ±1,5N·m

The procedure to find out the stiffness value is identical in both extension and flexion. Several assumptions were made in the theoretical calculus. First of all the compression force due to the bending moment was supposed to act in the middle of

25

every rubber piece and perpendicular to the vertebra. The shear force component is neglected to create bending moment. The bending moment together with the distance from the centre of the rubber to the rotation's centre of the lower vertebra determines the required force (Fig.3-6) to be applied on the rubber: 54.656N at flexion and 32.72N at extension
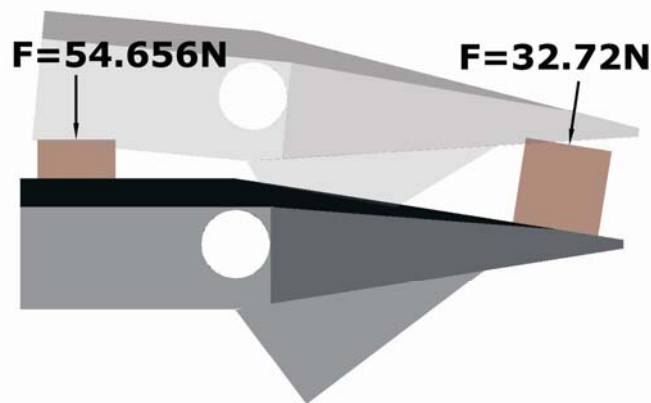


**Fig. 3-6** Values of forces to create the bending moment of 1.5 Nm at flexion and extension

Compression moduli, $E_c$, values were calculated for both flexion and extension, using Eq.2:

$E_c$ *Flexion*= 1174331.5508 Pa    $E_c$ *Extension*= 622080.687479 Pa

The rubber is just glued to the lower vertebra, therefore there is just one dimensional strain from the upper vertebra and it is possible to find out the value of these moduli with Eq 3. The shape factor, $S$, depending on the geometry of every piece is found out:

*S Flexion*= 0.5657    *S Extension* = 0.3370

It is computed the value of the Young's modulus:

$E_o$ *Flexion*= 677000 Pa    $E_o$ *Extension*= 421500 Pa

The rubber industry always defines the materials referring them to the hardness scale. The relation between hardness and Young's modulus (Fig.3-1) was used to calculate the equivalence shore A hardness for both values:

Flexion shore A 25º    Extension shore A 15º

### 3.2.1.3    Second approach: Real tests

rubber components used in the dummy were kindly given as a present from Lagomat AB. y were made from cast polyurethanes because of its good physical properties such as durability, good elasticity and wide range of hardness (stiffness) available.

In order to achieve high accuracy in the thickness of the rubber to set up the neutral position and because of the fact that cutting softer polymers is quite tough, a simple mould (Fig.3-7) was used to manufacture the polymer.
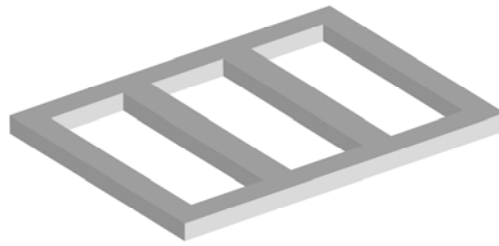
**Fig. 3-7** Real mould and 3D mould use to manufacture the rubber with the desired thickness

It comprises a square frame made by steel with some compartments; the thickness on each mould is the one required on every intervertebral space. A square glass is glued on the bottom part to achieve a smooth surface of the rubber. The polymers are made by two components: the prepolimer polyurethane and the cure system. Both of them are poured into the mould and then a glass is clamped on the top. It should be noted that the components should be vacuum before pouring them to avoid air bubble inside the material that would change their properties. Release agents should be used to spray both mould and glass in order to make easier to get the rubber out. To increase the speed of the vulcanize process; it is placed on an oven at 45ºC for a day. Due to the softness of the polymer on some test pieces it was necessary to use special tools to cut them into the desired shape. A high water jet pressure method was used to cut polymer pieces with hardness below 30 Shore A. All the final rubber components placed on the prototype were prepared with this method because, apart from being able to cut soft polymers, it also provides high accuracy and smooth surfaces.

Once the hardness value of the rubber piece was computed theoretically, two polyurethanes were moulded with their data: 25 Shore A piece of 4.5x8.9x14mm for flexion and 15 Shore A of 10x13x14mm for extension. The results from this first test were not satisfactory.
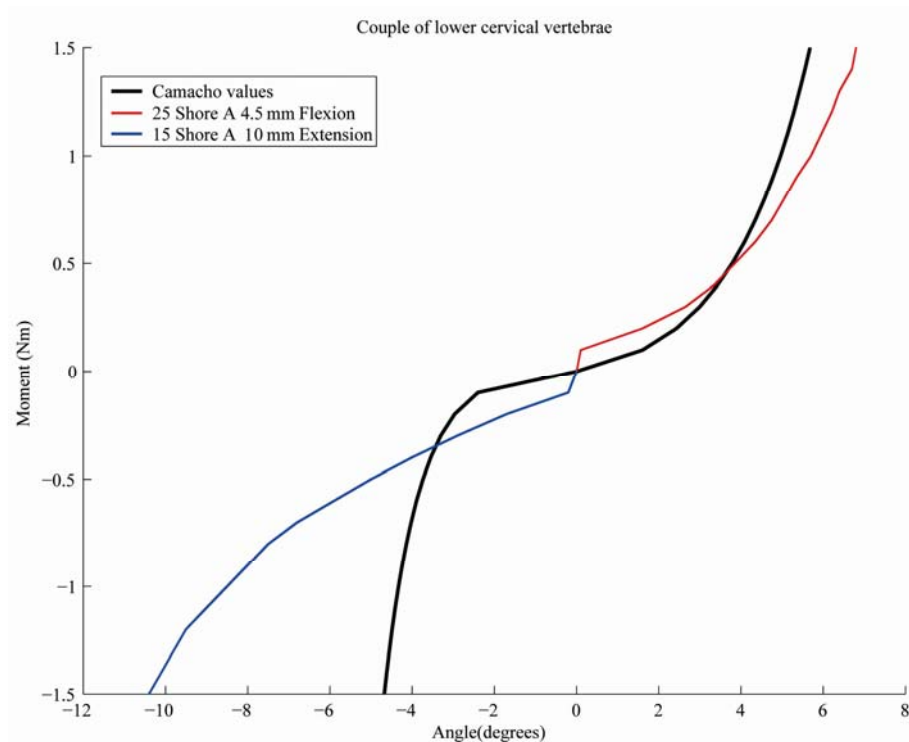


**Fig. 3-8** Test results with the theoretical hardness values of the rubber: 4.5x8.9x14mm for flexion and 10x13x14mm for extension

A really bad behaviour on extension is shown but it can be predicted due to the use of a methodology to calculate the hardness devise to long thin pieces of rubber, and the rubber piece for extension doesn't fit this criteria. The flexion rubber, which has a more suitable design, long and thin, displays a better behaviour but a bit softer.

Further tests (Fig.3-9) were performed increasing the hardness values of the rubber for both extension and flexion and changing the dimensions (keeping the thickness constant) of the polymer components. It was proved that the smaller the rubber pieces the softer behaviour they have, but size shouldn't be decreased too much from the initial values (9x14mm and 13x14mm) because their performance is unstable
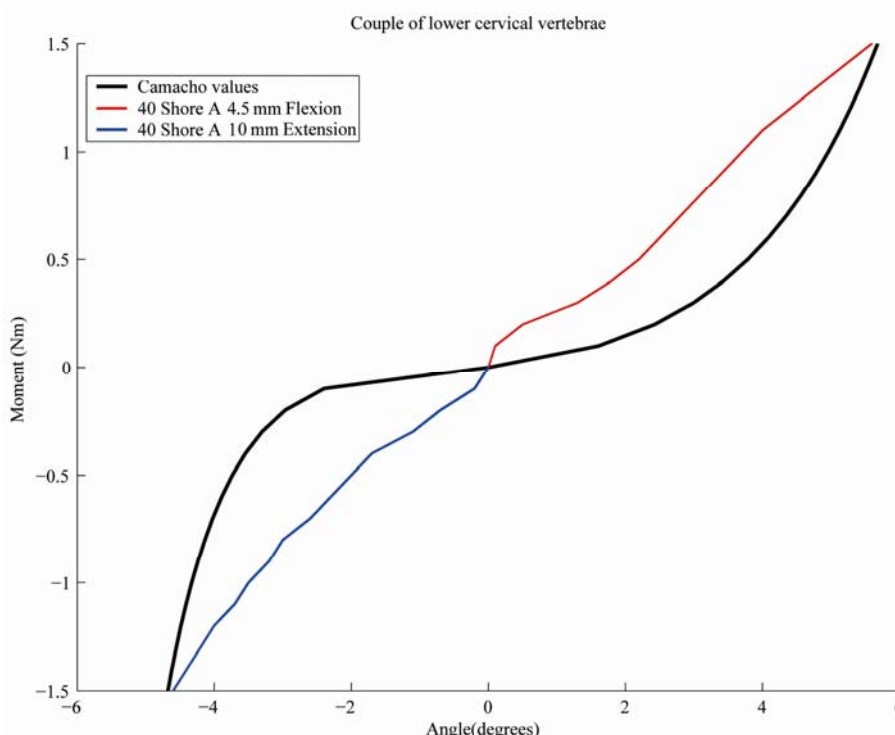


**Fig. 3-9** Test results with harder rubber pieces following a linear behaviour: 4.5x10x14mm flexion and 10x10x14mm

It is seen that these new values of the hardness agree better than the one tried before but the rubber has a rough linear behaviour in the range of the applied moments. As it was explained before, one of the most typical characteristics of the biomechanical structures is their non-linear behaviour with the growth of the stiffness as the applied load is getting bigger. In order to try to imitate this behaviour, new rubber components were moulded with a new method. It was used a two layer polyurethane, first layer imitates the stiffness of the neutral zone while another harder polymer replicates the range of motion stiffness. In order to get that, it was computed the amount of components required for every layer with the density and the volume of the mould to fill. The harder polymer was poured before in the mould and after its vulcanize process, the softer polymer was added. New adjustments and many tests were made before getting the right values of the hardness for every layer.
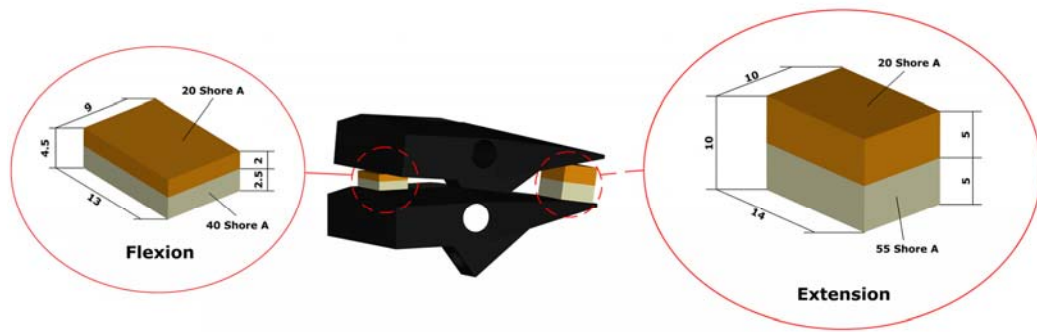
**Fig. 3-10** Rubber dimensions together with its hardness properties placed between vertebrae in the lower cervical

Finally, the results for the definitive chosen rubber for the model are shown (Fig.3-11). The rubber piece for flexion has a 9x13mm$^2$ area with 4,5mm of thickness which are made by 2,5mm layer 40 Shore A and another one of 2mm 20 Shore A. For extension a 10x14mm$^2$ rubber piece of 10mm thickness composed by a 6mm 55 Shore A and 4mm 20 Shore A layers was used.
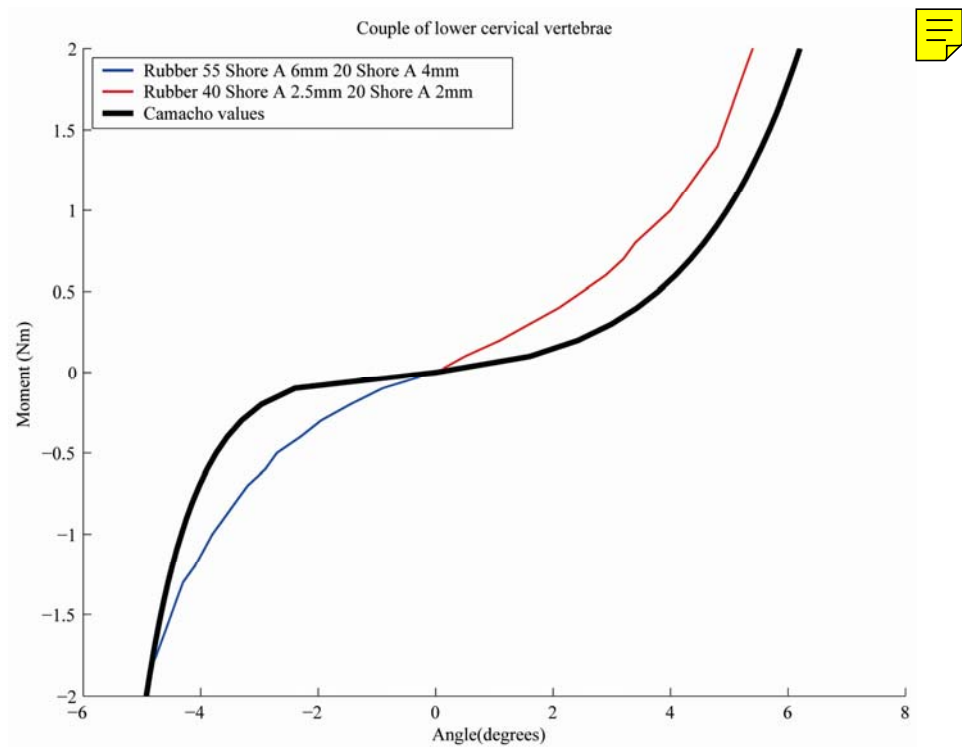


**Fig. 3-11** Final model values of the dummy neck rubbers in flexion/extension

As it can be seen on the graphic the test were extended to higher loads up to 2.0 N·m and the Camacho values were obtained assuming that Eq. 7 could be used for larger moments as well. The behaviour of the rubber resembles the human values with its particularities of hardening the stiffness as the load is increasing.

## 3.2.2 Coupled movement

The couple patterns in the lower cervical spine are one of its most important characteristics. On this part of the spine lateral bending movement is always coupled with axial rotation. Due to the symmetry about the sagittal plane of the spine, all values

for both displacements are referred to one side. The dummy neck replicates this behaviour; every movement in lateral bending has an axial rotation associated. Several studies on the lower cervical spine have been carried out: Goel et al. [13, 12], Moroney et al. [23] and Panjabi et al. [25, 26] It is seen that the data from Moroney et al. and Camacho et al. show a good correlation while the values from the other two authors have less stiffness properties; therefore Moroney et al. data were used to validate lateral bending and axial rotation of the dummy neck. Their study describes the static flexibility experiments on thirty-five adults' motion segments from sixteen cervical spine sections. Unfortunately available data from this test are not as detailed as in the Camacho et al. values and just average displacement for 1.8 N·m applied moment and stiffness obtained from linear regression are given (Fig.3-12).
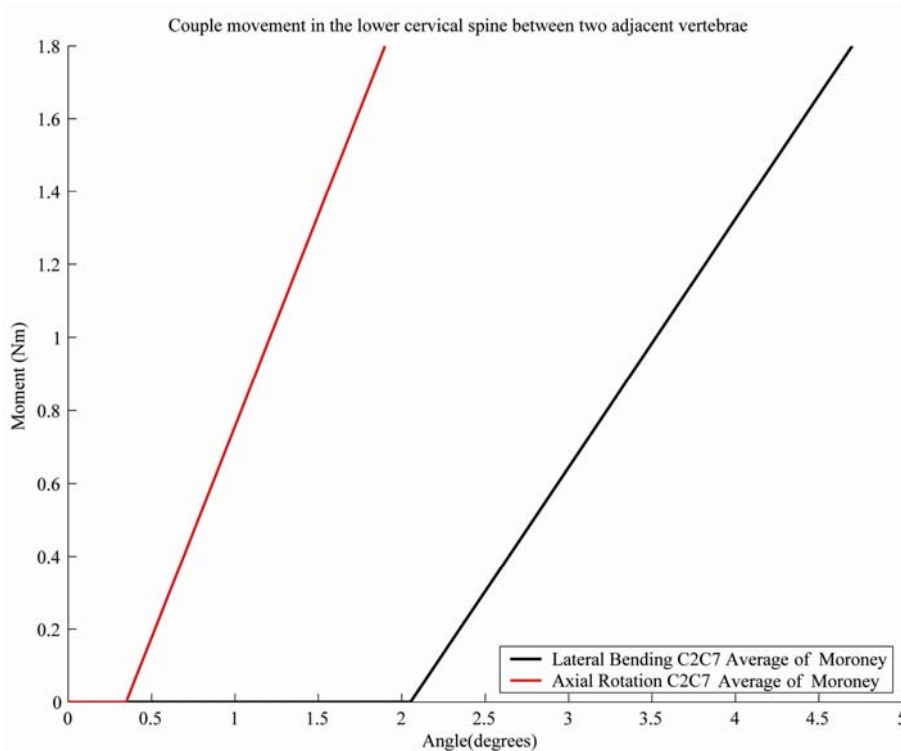


**Fig. 3-12** Reported average of Moroney et al. for lateral bending and axial rotation in the lower cervical spine Measurement instrument

The apparatus used to do measurements was the same that in flexion/extension but its position relative to the vertebrae was changed to measure lateral bending (Fig. 3-13).
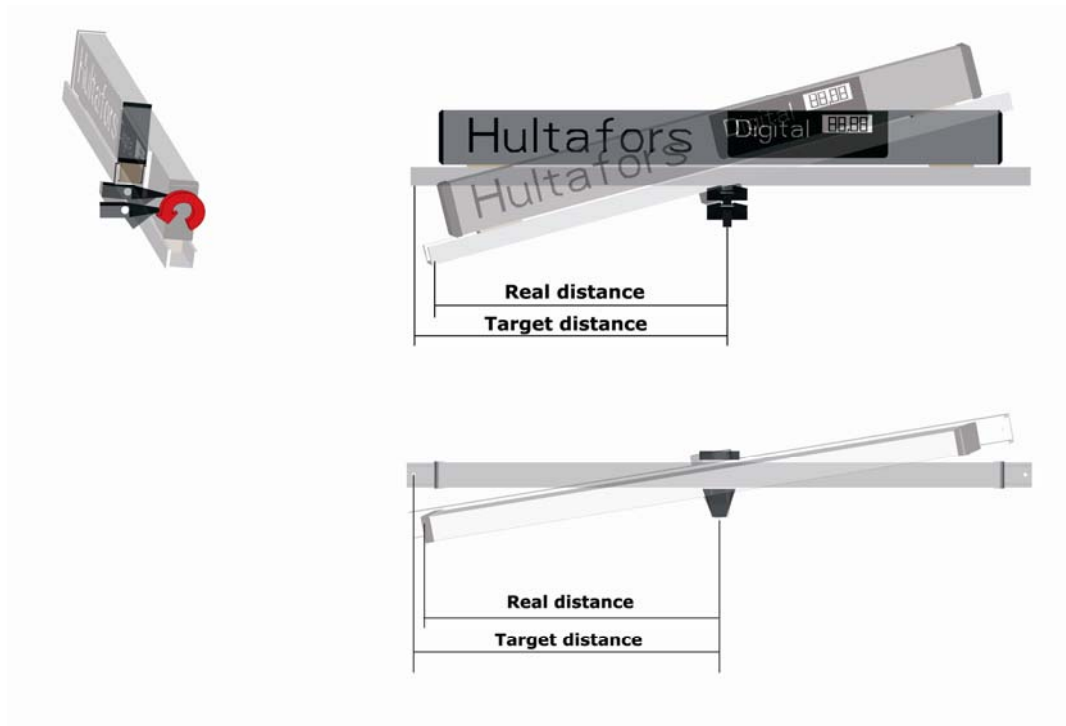
30

**Fig. 3-13** Location of the measuing instrument for lateral test and rotation produced in the goniometer

The deviation due to the decreasing of the distance from rotation's centre of the vertebra to hang weight is bigger on these tests because there are two sources of divergence due to the spatial orientation of the joints between vertebrae: one on the lateral bending direction and one on the axial rotation. The procedure to correct it was identical to flexion/extension just repeating the process twice.

Another problem arose because of the attach position of the goniometer and the particular design of the vertebrae. A rotation is generated around a transverse axis through the goniometer and the angle measure could be inaccurate (Fig. 3-13).

The technical specifications of the digital goniometer from Hultafors don't explain the alteration on the measurement of the apparatus when such rotations are produced, so an easy test (Fig. 3-14) was done with the goniometer to check the tolerance in the device.



**Fig. 3-14** Test performed to the goniometer to know the deviation in the measurements if a rotation of the device is produced

It was placed with a slope such the maximum angle (6º) would be obtained on the test to be performed, then a rotation was done around an axis through the goniometer up till 15º (maximum angle) on every side checking the measurements values. The tolerance of the device was just ±0.1º and it was verified the reliability of the acquired data.

### 3.2.2.1    Real test

A rubber was placed between vertebrae to get the stiffness in lateral bending and axial rotation. It should be noted that the flexion/extension rubber cushions restrict the movement a bit in the other two directions. There are two particularities that should be considered before defines the rubber. On one hand the slope of the lower vertebra on its sides, where it should be glued the rubber, makes inadvisable to choose a prismatic shape like in flexion/extension because it is impossible to get a good interaction between both pieces. It was selected a trapezoid shape (Fig.3-15) instead that fits perfect in the interverterbral space on the sides and has a smooth behaviour limiting the movements.
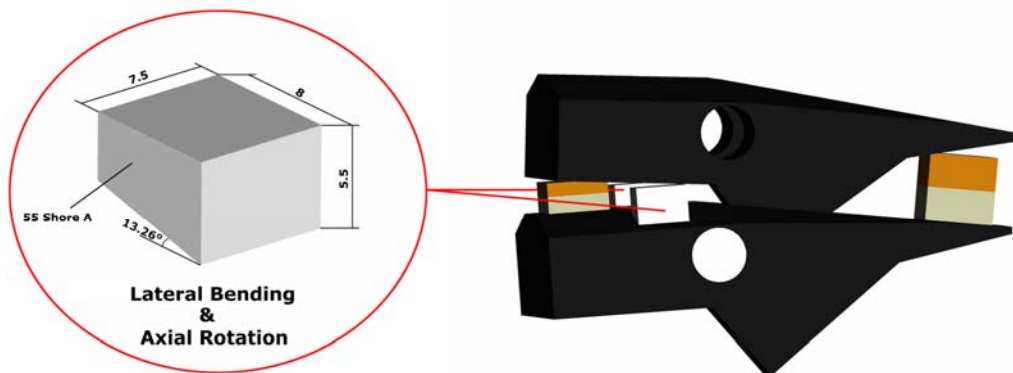


**Fig. 3-15** Rubber cushions to limit lateral bending and axial rotation of the vertebrae

On the other hand the design itself of the vertebrae and the mechanical solution taken with the screw to replicate the couple movement makes both displacements being directly related, so it is impossible to replicate the human values from Moroney et al. for each movement separately. With the aid of the CAD software it was found out the relation between lateral bending and axial rotation on the dummy neck: 1º of lateral bending creates 0.61361º of axial rotation while the data from the studies presents an average value of 1º of lateral bending produces 0.28665º of axial rotation. Therefore it is impossible to follow both of them in the model; the solution was to follow the lateral bending values from Moroney and afterwards axial rotation values were checked.

The previous experience from flexion/extension tests was used to determine the hardness. The final rubber pieces placed on the dummy are 55 Shore A hardness with 7.5mm thickness the trapezoid (8mm base, 5.5mm height, 13,26º angle). The tests were performed measuring the lateral bending (Fig. 3-16) response and it was converted afterwards to get the axial rotation.
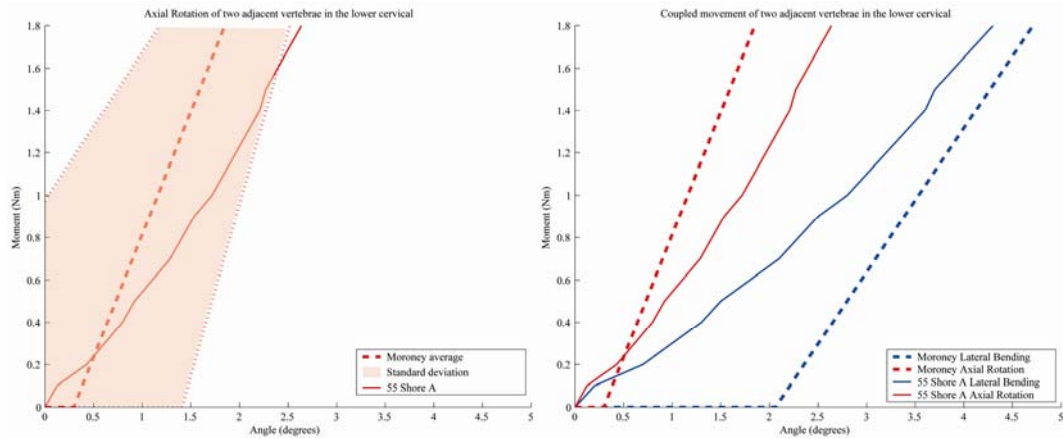
**Fig 3-16** Test results: coupled movement in the lower cervical spine

It is seen in the graphics that the values obtained for axial rotation are more flexible than in vitro values but they agree reasonable well inside the standard deviation of the experimental test. According to the test, the behaviour of the rubber resembles the human values with its particularities of load-displacement curve (hardening the stiffness as the load is increasing), like in flexion/extension.

## 3.3 UPPER CERVICAL

The moment-rotation characteristics of the upper cervical spine are documented for static loads. They were determined by Goel et al. [14], Oda et al [24], Panjabi et al. [33, 34, 35] and Camacho et al.[2]. The experiments used a similar set-up: pure moments were applied to the upper most vertebra while the lowest vertebra was fixed and three-displacement were measured in flexion/extension, lateral bending and axial rotation. But there were differences between studies like number of specimens, group of them to test (C0-C5 Goel, C0-C3, C0-C7 Panjabi and Oda or C0-T1 Camacho) and range of applied moments (0.3N·m Goel and 1.5N·m in the rest of them). Because of the fact that the neck was devised to fit the whole population the average values of all studies were taken as pattern.

### 3.3.1 Flexion and Extension

The data from Camacho et al. were used in the lower cervical spine to define the intervertebral properties of the dummy so as to do the right thing and to preserve uniformity in the stiffness characteristic; they were applied in the upper cervical part of the prototype too. Due to difficulties in visualizing C1 during testing, the C0-C2 complex was treated as a single motion segment in the experiments and there were no available data for each couple of vertebrae. In order to overcome this problem, the available data from other experiments were used to identify the contribution of every couple of vertebrae (C0C1 and C1C2) to the whole movement of the upper cervical. Because Oda et al and Panjabi et al used a similar experimental set-up and a maximum moment of 1.5 N·m to determine the ROM, their data may be pooled and averaged, furthermore the range of applied moments in both studies is the same as Camacho test. It was computed the average of Oda and Panjabi values of ROM and the percentage of whole flexion and extension of the upper spine that matches with every couple of vertebrae.

| | C0C1 | C1C2 | C0C2 | % C0C1 | % C1C2 |
|---|---|---|---|---|---|
| Flexion | 10.2º | 11.7º | 21.9º | 46.57 | 53.43 |
| Extension | 16.3º | 9.6º | 25.9º | 62.93 | 37.07 |

The Camacho values from C0C2 were divided with these proportions into C0C1 and C1C2.
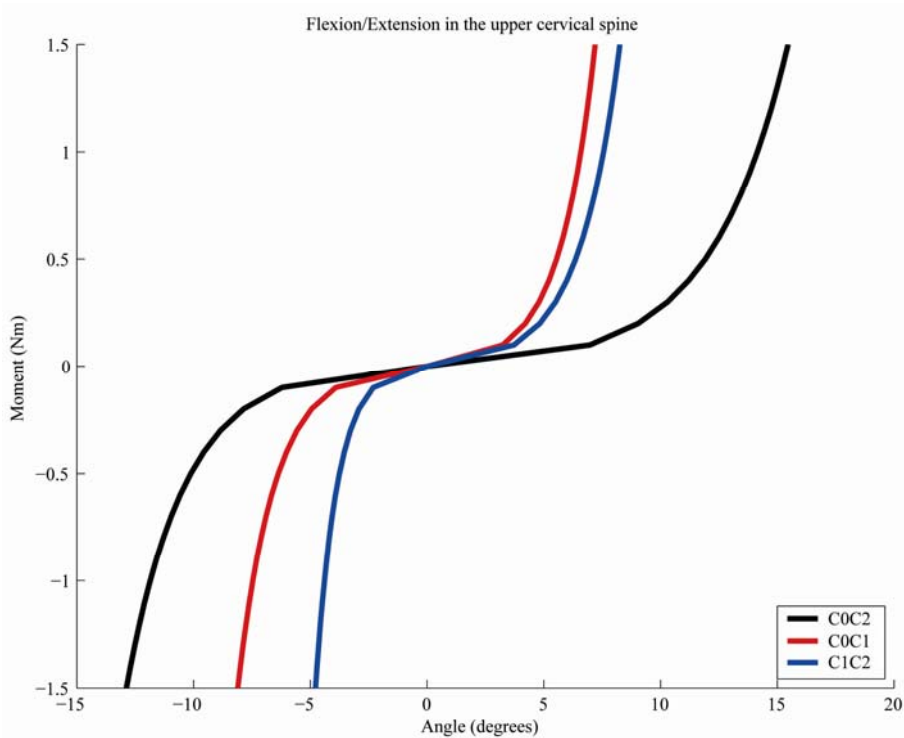


**Fig. 3-17** Camacho values for the whole upper cervical spine and contribution of every couple of vertebrae

As it was done in the flexion/extension design of the lower cervical, the dimensions of the rubber between C0C1 and C1C2 should fit perfect in the intervertebral space and hold the neutral position of the neck in the upper cervical. With the aid of the 3D model of the pieces, the space between them was found out for both couple of vertebrae in flexion and extension.

**Table 6** Intervertebral space and rubber dimensions (mm) in the upper cervical

| | Intervertebral space | | Rubber dimensions | |
|---|---|---|---|---|
| | C0C1 | C1C2 | C0C1 | C1C2 |
| Flexion | 8.47 | 9.63 | 9 | 10 |
| Extension | 12.73 | 7.14 | 13 | 7.5 |

34

### 3.3.1.1 C0C1

**Measurement Instrument.** The device to measure the relative displacement of these two vertebrae in flexion and extension is based on the lower cervical one with some modifications (Fig.3-18) to fit into C0.
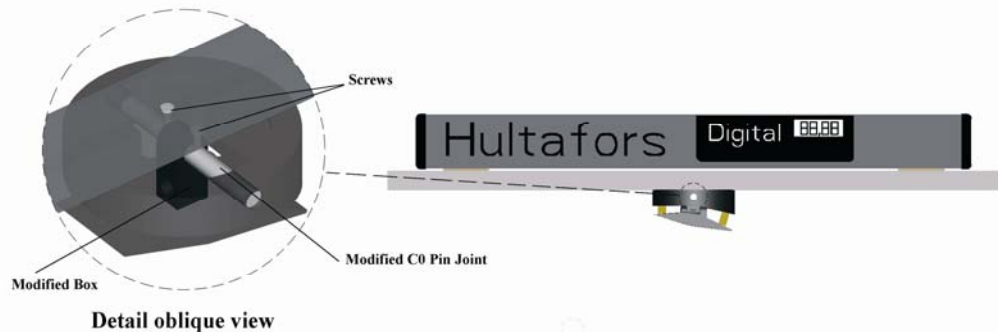


**Fig. 3-18** Measurement device for flexion/extension between C0C1 together with a detail view of the modifications done

The box that connects C0C1 is replaced with a new box with the lower part flat instead of round off to avoid lateral movement between vertebrae so just flexion/extension is permitted during the test. The normal pin joint that attaches C0 to the head and the box is swapped by a new one with two holes next to the sides of the box. Two holes with the same diameter are drilled in the aluminium profile and the measurement instrument is fixed on the top of the C0 thanks to two screws going through it. It should be noted that the deviation in the measures that was explained in the former chapters has its maximum level, but it was corrected following the same procedure with the new distance and the cosine of the angle as it was described before.

**Real tests.** Rubber pieces (Fig. 3-19) were placed between C0 and C1 too, but in these two vertebrae unlike lower cervical the rubber is glued to the upper vertebrae instead of the lower one because of the C1's shape. C1 has a cleft on its frontal top surface to allow the pin joint to connect the box to the vertebra; therefore it is inadvisable to glue the rubber to this side.
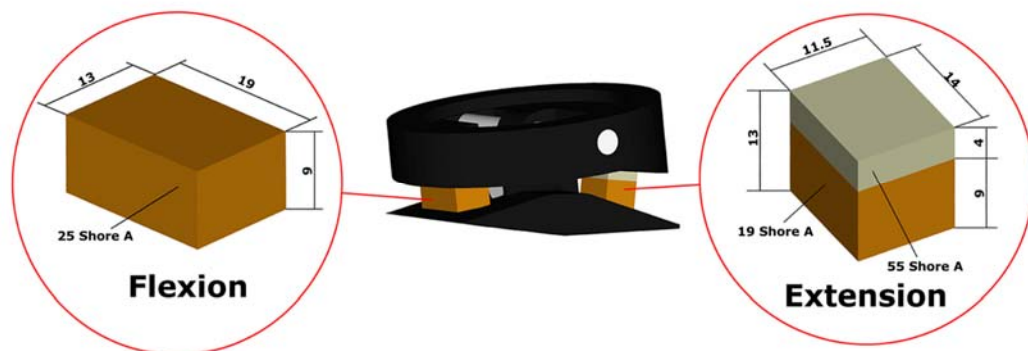


**Fig. 3-19** Rubber cushions placed between occiput interface and C1 for flexion/extension

Several tests with different rubbers and sizes were performed until reliable values were found out. The final rubber piece for extension is a two layer polymer of 13mm thickness and 14x11.5mm$^2$ area with a 9mm layer of 19 Shore A hardness and a 4mm

layer of 55 Shore A. A 9mm thickness and 19x13 mm$^2$ 25 Shore A was chosen for flexion.
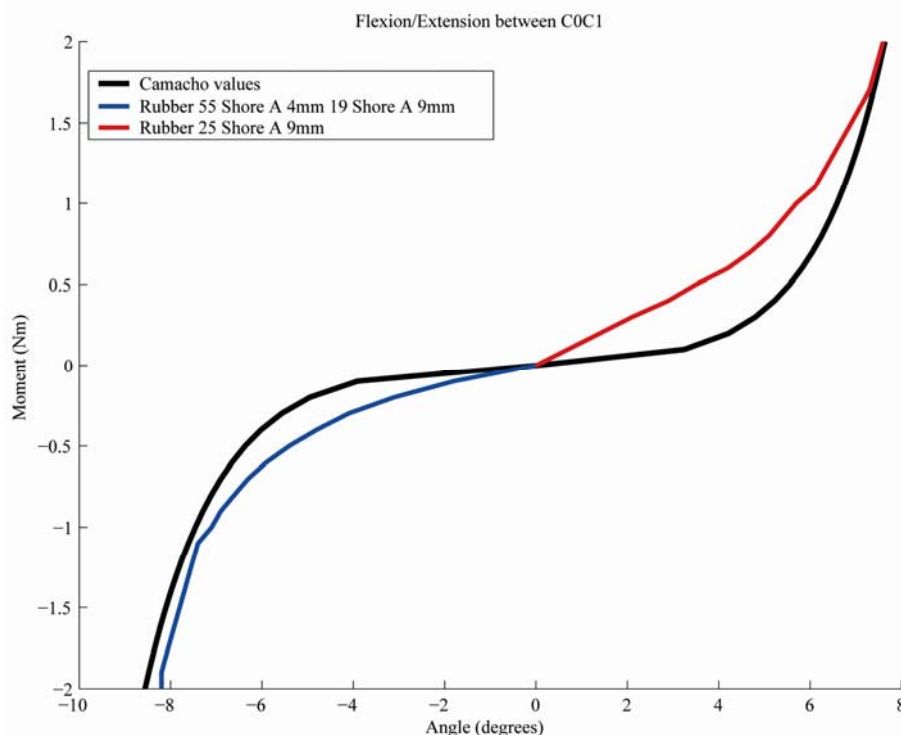


**Fig 3-20** Final values of the dummy neck rubbers in flexion (positive)/extension (negative) between C0C1 together with Camacho values

The tests were extended to higher loads up to 2.0 N·m showing a really close behaviour to the human values.

### 3.3.1.2   C1C2

**Measurement Instrument.** The device to measure the relative displacement of these two vertebrae in flexion and extension is based again on the lower cervical one (Fig. 3-21).



**Fig. 3-21** Measurement device for flexion extension between C1C2

The modified pin joint is placed on the hole through the two jut out parts of the C1 where it should be the pin joint to connect with the box and C0. The device leans against these two parts. The test apparatus has two deviations in the measurements: on one hand the one due to the angle and the decrease of the distance as it was explained before and on the other hand the because of the fact the centre of rotation from the lower vertebrae and the centre of the device are misaligned. The distance from the rotation's centre to the weights is different in flexion (smaller) and extension (bigger).

Both deviations were corrected carrying out the real distance from the centre to the weight once the load is applied for every moment.

**Real test**. The rubber cushions were glued on the lower vertebra, C2. In order to not to interfere with the axial rotation movement between these two vertebrae that will be described later, a thin layer of plastic film, like the one used for cooking, is placed on top of the rubber to avoid the friction produced between the polymer and C1.
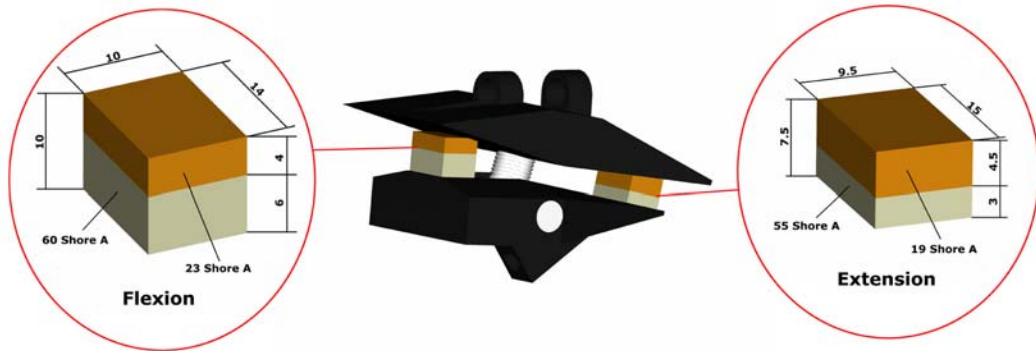


**Fig 3-22** Rubber bumpers located between C1 and C2 vertebrae of the dummy

The flexion's one is a two layer polymer 10mm thickness and $14 \times 10 \text{mm}^2$ with a 6mm 60 Shore A layer and 4mm 23 Shore A hardness while the extension is 7.5mm thickness $15 \times 9.5$mm with one sheet 3mm 55 Shore A and 4.5mm 19 shore A.
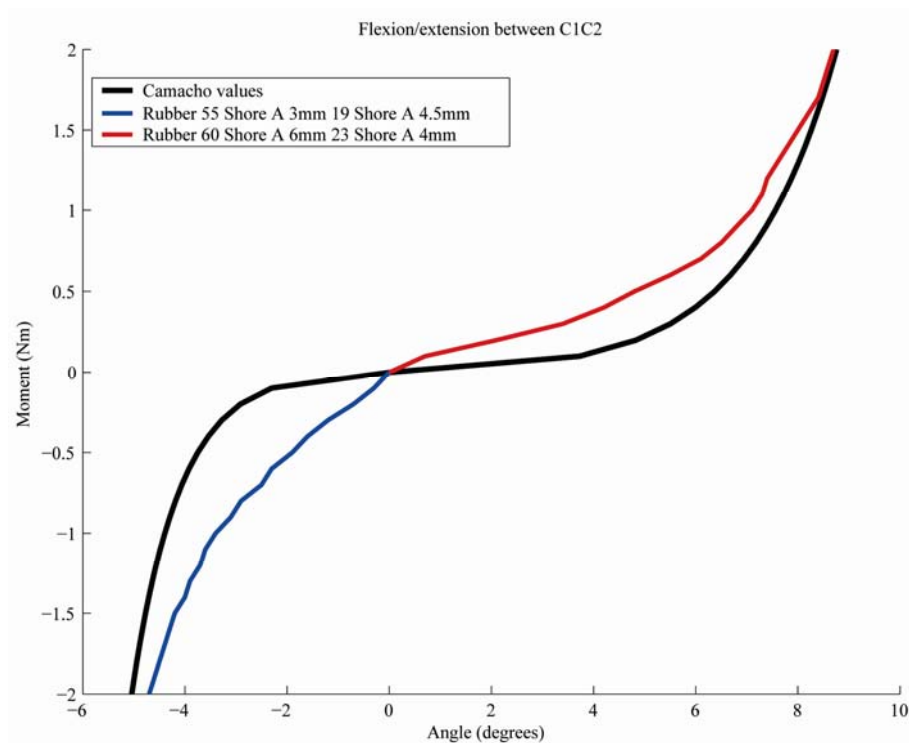


**Fig. 3-23** Final values of the dummy neck rubbers in flexion (positive)/extension (negative) between C1C2 together with Camacho values

The tests show that both rubbers replicate quite closely in vitro values.

## 3.3.2 Lateral Bending

In order to simplify the design of the neck the lateral bending between C1C2 was neglected [31], therefore it just appears between C0C1 by means of the box that connect them. From all available studies for lateral bending, the average values(Fig. 3-

24) from Panjabi et al [33, 34, 35] and Oda et al. [24] were taken to define the stiffness properties because their similarities to the other studies used before in the other parts of the dummy (analogous set up and load:1.5N·m).
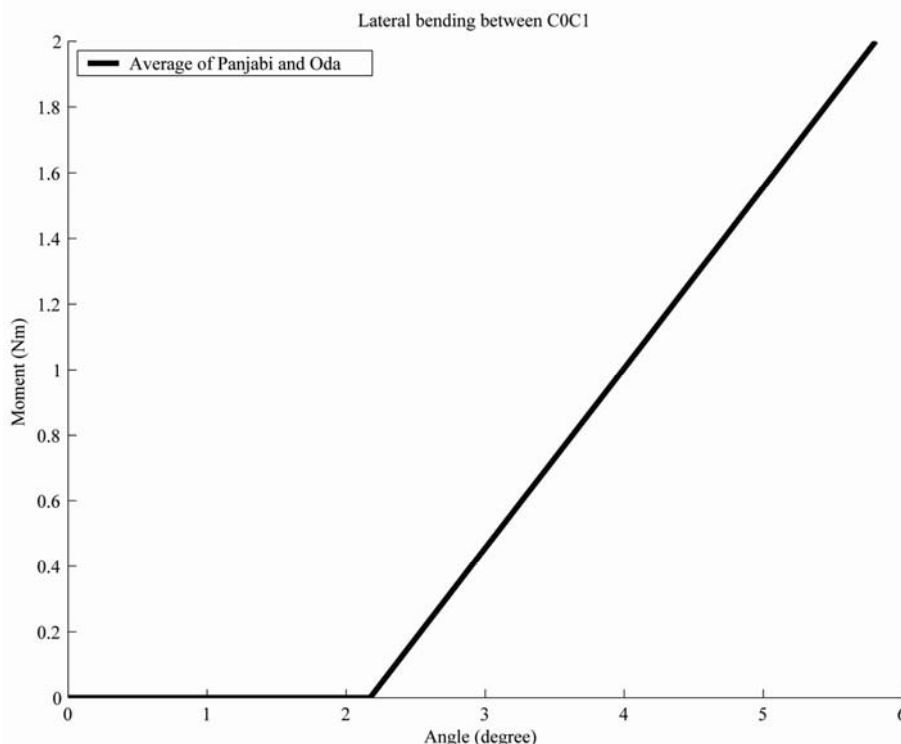


**Fig. 3-24** Average of Panjabi et al [33, 34, 35] and Oda et al[24] values for lateral bending between C0C1

Anyway, it should be noted that a general comparison between experiments shows a less stiff behaviour than the ones from Camacho and Moroney. Although these data provide more flexible values, the behaviour of the whole neck is compensated somehow due to the fact that C1C2 lateral bending was neglected.

**Measurement Instrument.** The apparatus to measure the displacement between these two vertebrae in lateral bending is based on the lower cervical one with some modifications. The range of lateral bending moment between C0C1 is delimited by C1 and the neck load cell of the BioRID, which the prototype is attached to the head.
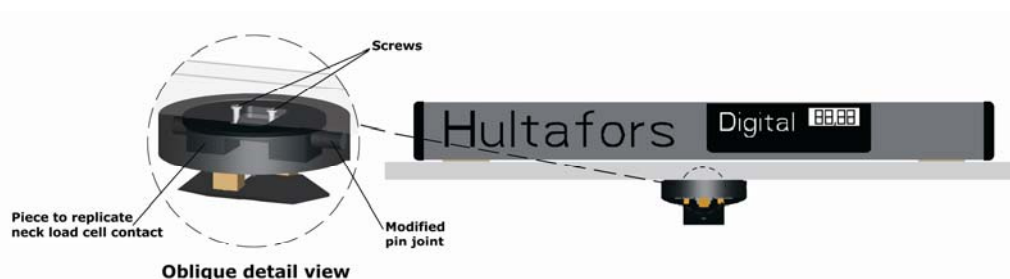


**Fig 3-25** Measurement device for lateral bending between C0C1 with a detail view of the new components

In order to be able to reproduce this contact, a new piece (Fig.3-25) that replicates the lower part of the load cell was manufactured. It has circular shape on the top to fit into C0 leaving enough space to lean the aluminium profile and two jut out parts in the bottom to imitate the load cell. A hole through the entire piece has been drilled to have

space for the box and the screws to fix the device. The assembly of the apparatus is identical to flexion/extension test of C0C1 (with the same screws and modified pin joint) apart from the placement of the device relative to the vertebrae. The deviations in the measurements due to the angle are quite small in this test but they are corrected as it was explained before.

**Real tests.** Two rubber pieces were glued on each side of C1. Both of them are identical 10mm thickness 9x14mm$^2$ made by a polymer 65 Shore A hardness with the following behaviour:
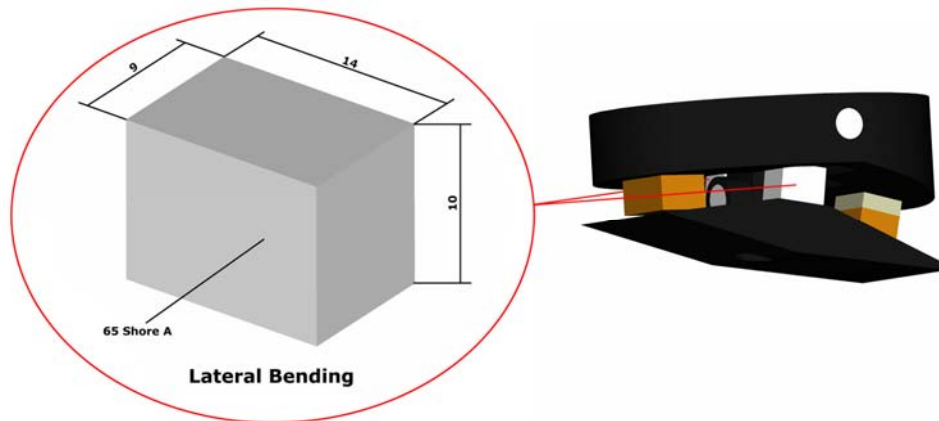


**Fig. 3-26** Rubber pieces placed between the modified load cell and C1

The results of the test with the rubber placed between vertebrae together with the data from Panjabi and Oda are plotted:
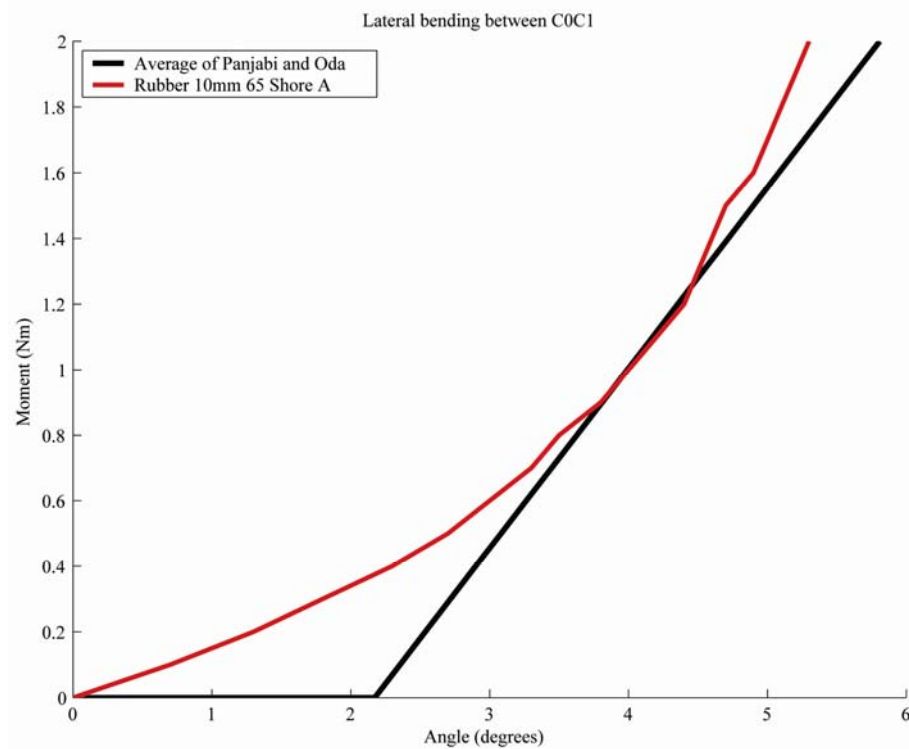


**Fig 3-27** Final values of the rubbers in lateral bending between C0C1 together with an average of Panjabi and Oda

### 3.3.3 Axial rotation

As it was mentioned before, the axial rotation between C0C1 was neglected in the upper cervical spine to make the design of the dummy easier, it just appears between C1C2. An average (Fig. 44) from Panjabi et al [33, 34, 35] and Oda et al. [24] values were used to define the stiffness properties as it was done in lateral bending between C0C1.
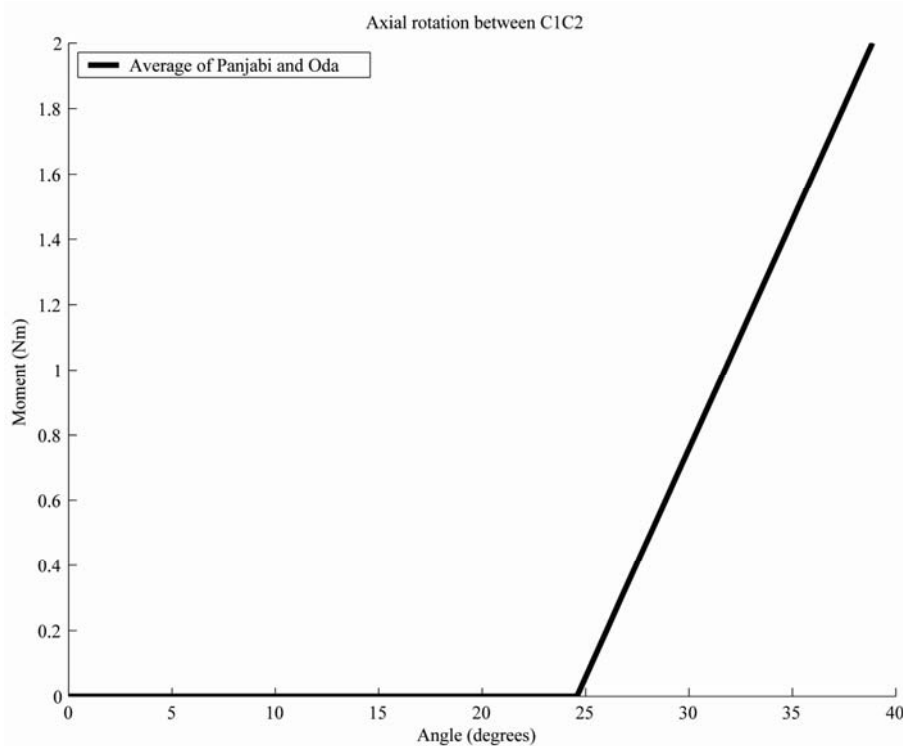


**Fig 3-28** Average of Panjabi and Oda values for axial rotation between C1C2

### *3.3.3.1    Cable*

In order to restrict axial rotation in the upper cervical spine a different solution than rubber was found out: a system based on a cable and its stiffness properties. The rope should be placed somehow that delimits the movement independently from the flexion/extension between vertebrae. It is fixed in one side to the pin joint between the vertebrae and in the other side to C1 (Fig. 3-29).
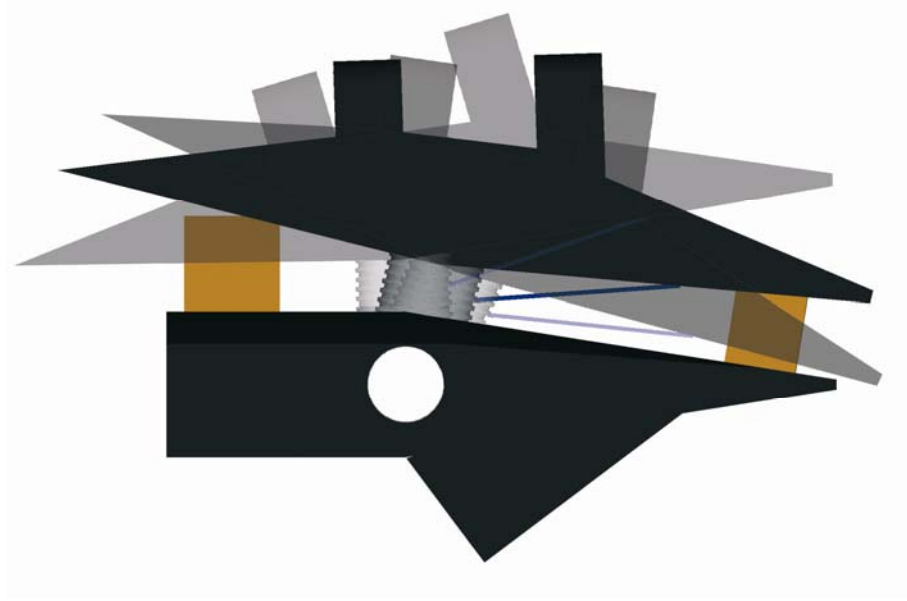
**Fig. 3-29** Position of the cable between vertebrae, its elongation is not affected by flexion/extension movement

Although some flexion/extension movement takes place between vertebrae, with this particular location (link to the pin joint and to C1) the tensile behaviour of the cable remains identical for every possible position because it moves together C1 around the pin joint of the lower vertebra.

**Theoretical approach.** The axial rotation between C1C2 is constricted by the elongation of the cable. When C1 rotates around the pin joint, the cable should stretch because the distance between the two fixing points increases from the initial value (Fig. 3-30).
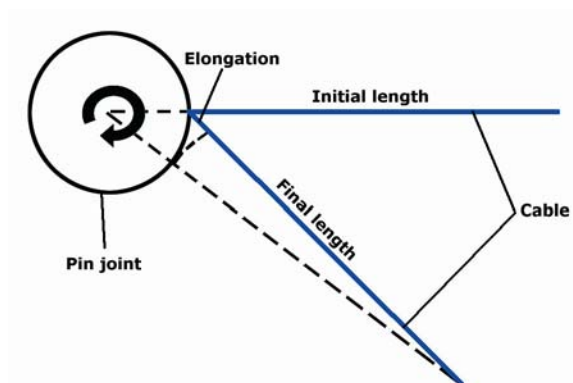


**Fig. 3-30** Elongation of the cable due to the applied moment between C1C2

From the applied torque it is possible to find out the tension that determines the stretchablity of the cable using simple geometry and trigonometry relations.
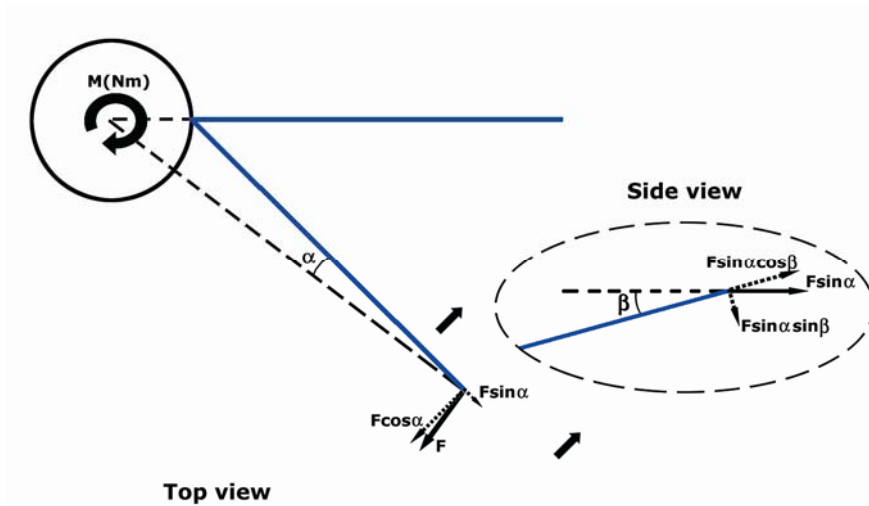
**Fig 3-31** Force components due to the applied moment

The moment creates a force (Fig. 3-31) in one end of the cable that it can be divided into one perpendicular and another parallel to it by means of the cosine and sine of the angle α (angle between the cable and the line that connect the rotation's centre with the end of the cable, projected over a plane perpendicular to the pin joint). Once the force is defined on a plane containing the cable, it is possible to compute the value of the tensile force of the cable using angle β (angle between the cable and a plane perpendicular to the pin joint) to break it down into shear and tension.

With the aid of the 3D CAD model of the dummy neck, it was figured out the values of these angles and the length of the cable for the axial rotation displacements of C1 from the average of Panjabi and Oda studies. Using these angles the applied moment can be transformed into the tensile force that acts on the cable for every position. Adding the elongation to these data, the required stiffness properties (Fig.3-32) of the rope are defined.
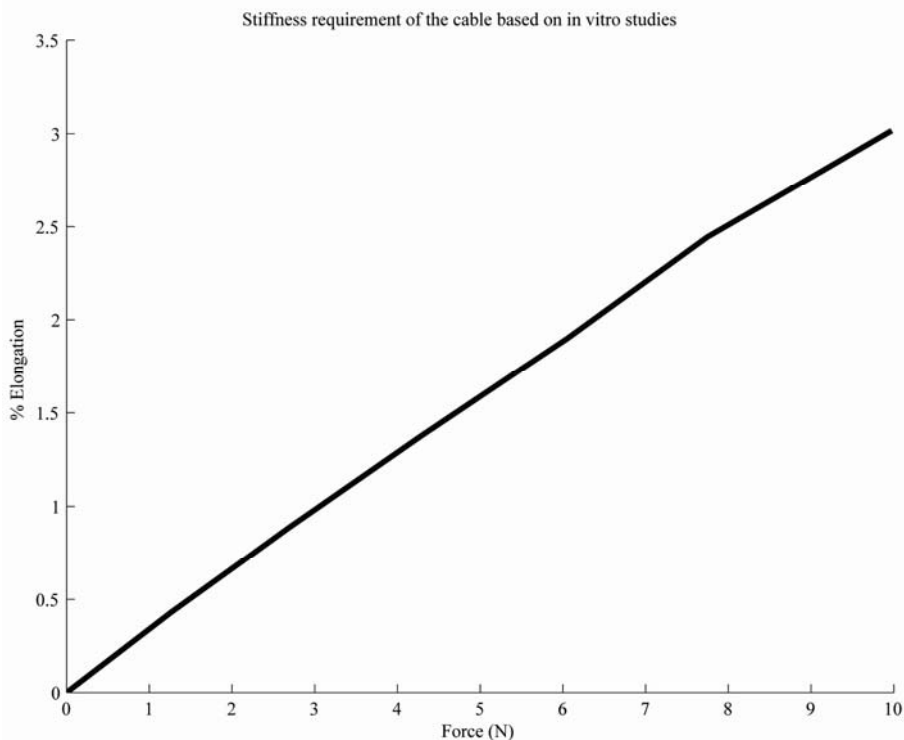


**Fig. 3-32** Tensile properties of the cable based on the values from Panjabi and Oda

The chosen material for the cable has been nylon, because its elasticity is closed to the required values. Several nylon cables with different diameters were tested. Due to the small length of the cable in the neck (21.5660mm), it was difficult to make the tests with the real vertebrae and measure the extension of it. To avoid the problem, simple tests (Fig. 3-33) on a bigger scale were performed.
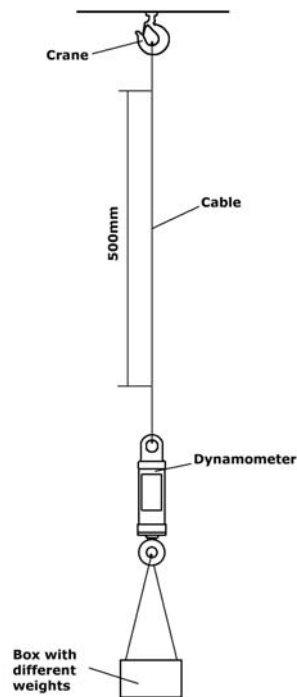


**Fig 3-33** Test set-up to calculate the elongation characteristics of every cable

Each nylon specimen was hung together with different weights; two marks with half meter distance between them were done on the cable and the increase of the distance was measured.

The values that agree better with the desired stiffness properties were found out with Ø0.45mm nylon cable (Fig. 3-34) that should be 21.56mm length while the distance between the two fixing points of the nylon is 21.09mm.
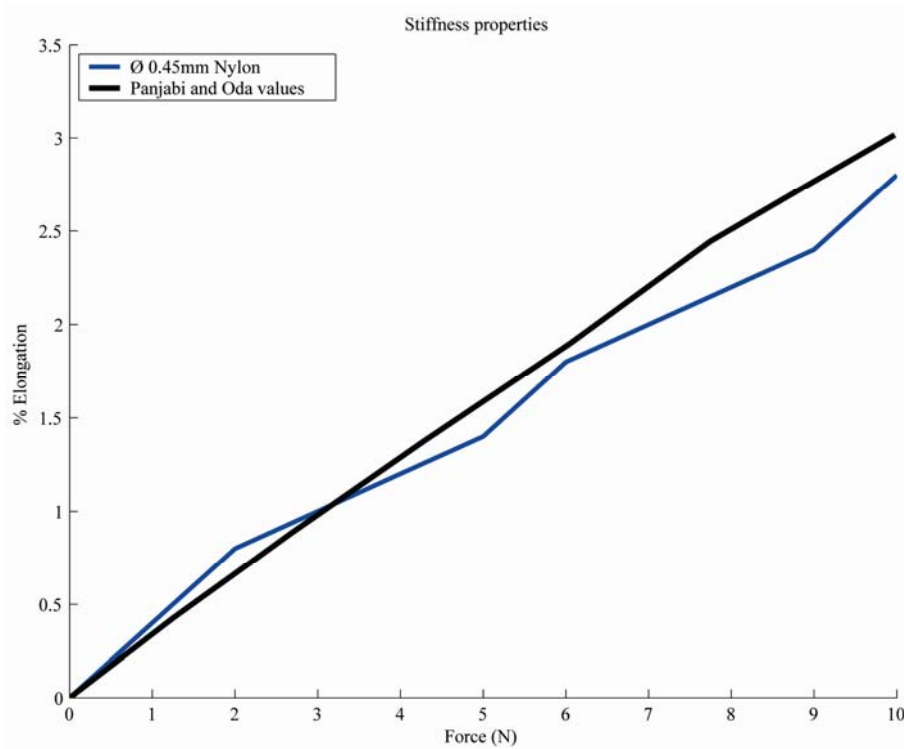
**Fig. 3-34** Stiffness properties of the chosen cable together with the target values from Panjabi and Oda

It should be noted that the nylon doesn't have a perfect elastic behaviour so a small permanent deformation comes out. After the tests were perfomed, the increase of the distance from the initial value of 500mm was measured. A 0.1% of permanent elongation that defines the deviation of the results was found out.

It is possible to predict the theoretical behaviour of the cable with a length of 21.56mm in the vertebrae in terms of Moment-Angle (Fig. 3-35) by means of repeating the process explained before in inverse order.

44

**Fig. 3-35** Theoretical values of the cable in axial rotation between C1C2 together with an average of Panjabi and Oda

**Real model**. Due to the small length of the cable, it is really difficult to get an accuracy of 21.5660mm; therefore a system for adjusting the tension of the cable in the ve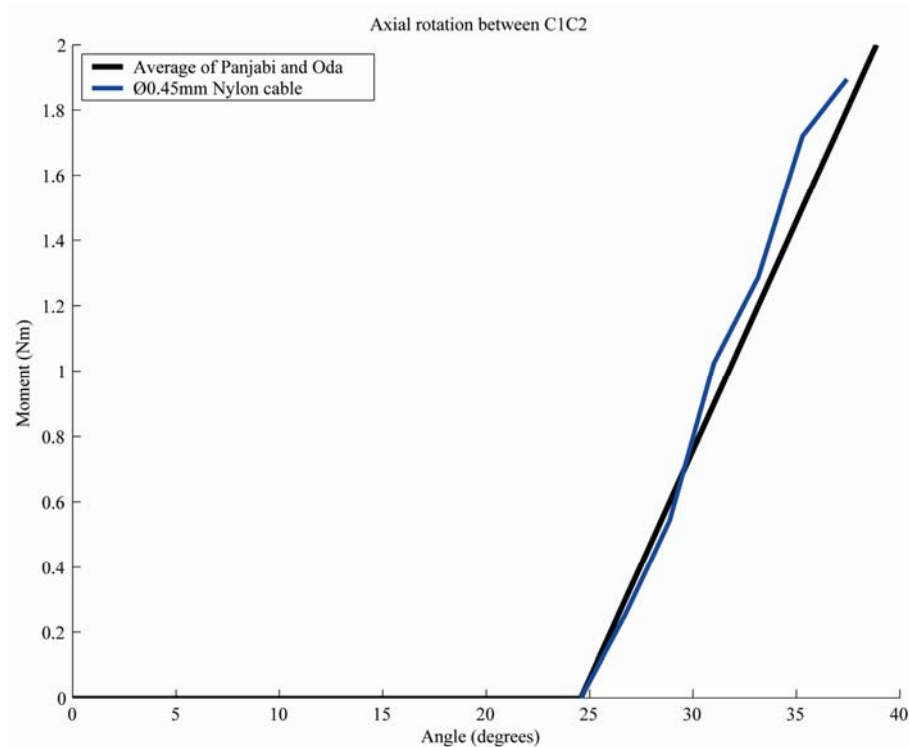rtebrae was the chosen alternative method (Fig. 3-36) used to define the stiffness properties in axial rotation between C1C2. On one side the cable is fixed to the lower part of C1; three holes were drilled: two in the bottom surface of the vertebra and a thread one on the side. Then the cable goes through the two bottom holes and it is fixed by means of a screw that presses it, being able to adjust the tension of the nylon. On the other side, it is fixed to the screwed part of the pin joint that connects C1 and C2. A hole with two different internal characteristics is drilled through the entire pin joint. On one side it is thread to allow inserting a screw that has in turn, a hole in the middle to let the cable go through it. By the screw movement it is possible to adjust the cable length.
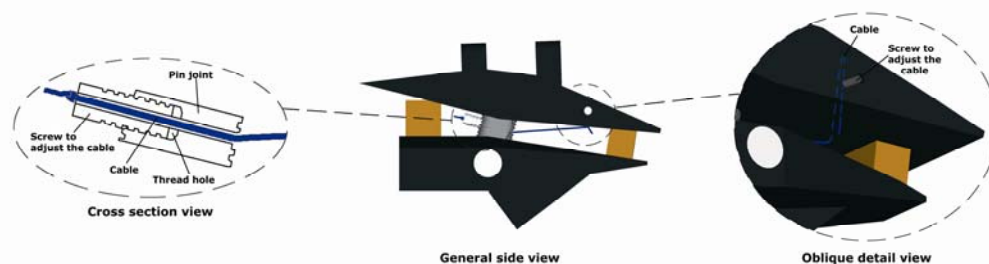


**Fig. 3-36** Methods used in the dummy neck to adjust the tension of the cable between C1C2

Due to the fact that the precision of the theoretical value is really difficult to get, the previous described system would be used to adjust the stiffness properties of the neck. The real test with the vertebrae could be done varying the cable length. For example, if the test shows a softer behaviour, the cable would be more stretched until the desired values are obtained.

45

# 4. CONCLUSIONS AND RECOMMENDATIONS

## 4.1 GLOBAL MODEL AND CONCLUSIONS

The final aspect of the global neck adding all the items described previously would be as follow.



**Fig 4-1** Global OmniDirectionalDummy neck II: manufacture prototype and 3D model

The neck fits into the head of the BioRID by means of attaching the occiput to the neck load as it is shown below.
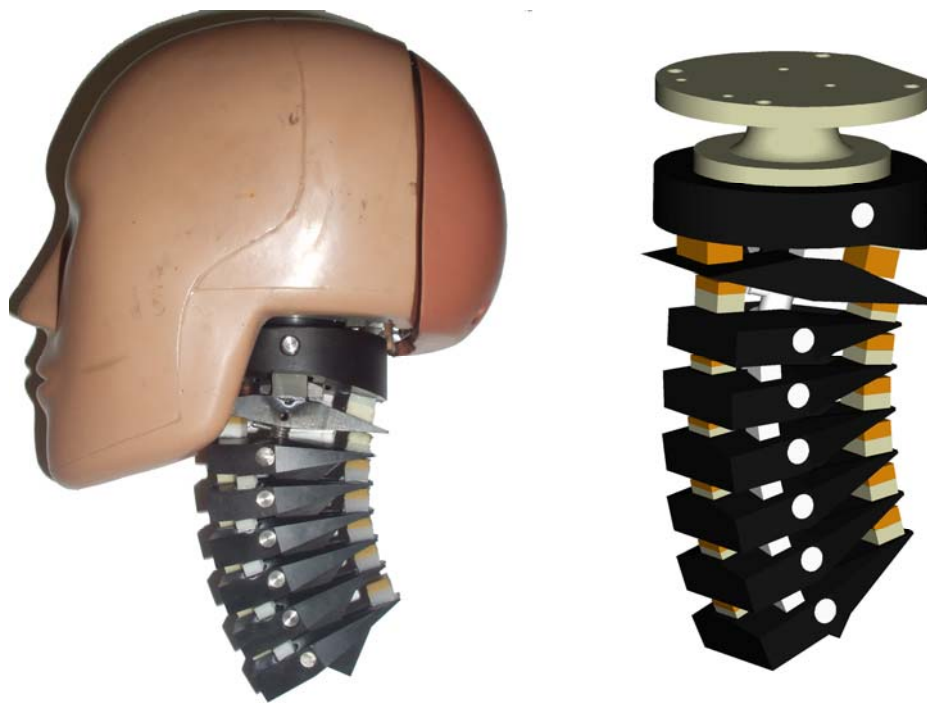
**Fig. 4-2** Real prototype attached to the BioRID head and global 3D model together with the modified neck load cell on the top

The static behaviour of the neck for the four main movements: flexion, extension, lateral bending and axial rotation are plotted (Fig. 4-3). It is shown that they agree reasonably well with the typical curves from the biological structures for all movements but axial rotation. The reason to this deviation in the values is that the main contribution to the global axial rotation happens between C1C2 and the results obtained are theoretical. However, it would be possible get a smoother curve closer to the human behaviour by means of varying the length of the cable or adjusting the pretension of the cable until the displacement between vertebrae follows a biofidelic pattern.

**Fig. 4-3** Static response of the ODD II dummy neck in the main four movements of the neck

The aim with this work was to develop a mechanical neck representing the skeletal cervical spine and all its movements in any direction. ODD II, this new three dimensional dummy neck 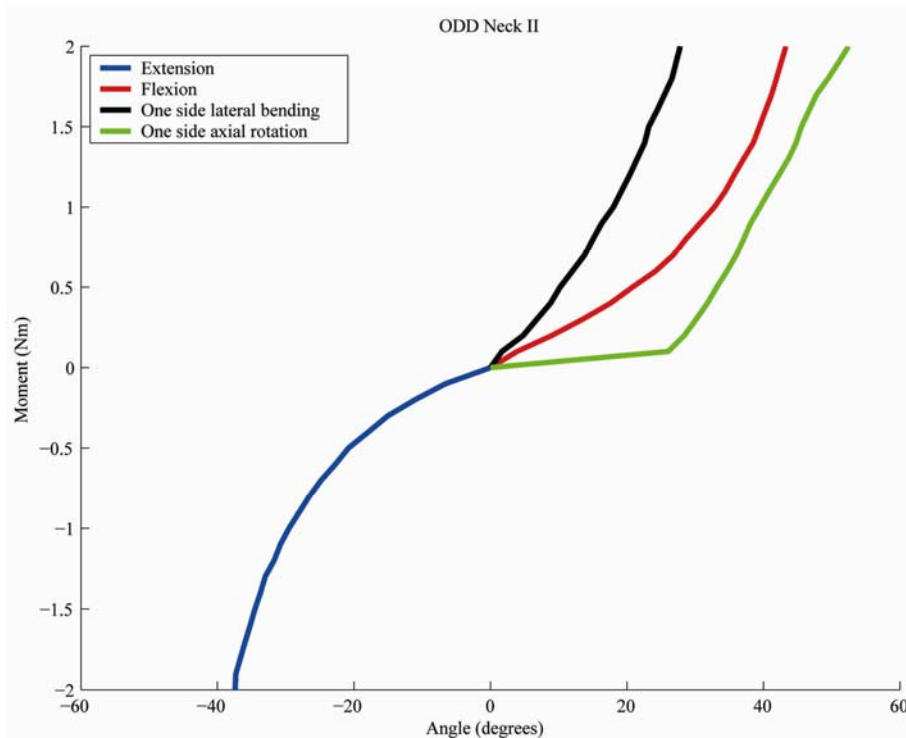not only does it replicate the movement pattern, furthermore, it has a biofidelic performance that closely simulates the behaviour of the human neck both range of motion and stiffness.

A main improvement is that it would be applied in lateral, oblique, roll-over (where the vehicle is vaulting), far side (on the opposite side of the dummy), frontal and rear-end impacts. It can also be seen as a complementary to the robust and simple crash dummies mostly used.

Although aspects like damping and dynamic properties, durability and repeatability were not studied in this thesis, the prototype represents a good basis for further studies in multidirectional dummy necks.

## 4.2 RECOMMENDATIONS

Taking this work as a good base of a dummy neck for multidirectional applications, there are suggestions to think about in further related studies.

In order to complete the static analysis of the dummy, a study of the axial rotation movement between C1 and C2 should be performed. A system to measure the response of the vertebrae to different moments must be designed. With the aid of these results it would be possible to define the pretension in the cable system adopted to follow human pattern.

All the dummy design and test have been done on a static basis, thus some dynamic test with the dummy, like pendulum test, should be completed in order to check the behaviour of the prototype and compare it with other dummies and human values. The last step would be performing real crash test.

48

The muscle response was neglected so a simulation of the human neck muscle and ligaments system could be implemented between vertebrae. There is probably no space in the prototype to replicate the whole muscle and ligaments system of the human neck but based on literature review, the main ligaments and muscle that has a greater influence in the neck response could be reproduced by means of cables placed between vertebrae as they are in the real human body.

Some movements were neglected in the upper cervical part of the dummy, specifically axial rotation between occiput and C1 and lateral bending between C1 and C2. The former one could be reproduced by means of changing the lower pin design and its position inside the box that connects both pieces. The surface of the pin would be threaded together with the hole in the box and the spatial orientation of the hole is changed from a horizontal position to a certain angle; therefore a lateral bending and axial rotation movement would appear as it happens in the other joint system. The latter dismissed movement could be obtained fastening the pin joint to C1 with an angle, it would be possible to find out the value that would create the coupled lateral bending and axial rotation movement close to the human values. Afterwards, a verification of the geometry of the vertebrae and their possible contacts between them together with the new range of motion for every movement should be performed on each case, as it would be necessary to change the design of the parts to follow the human displacement pattern.

The biofidelity in the lower cervical part of the dummy is liable to be improved. All the vertebrae were designed identical in shape and range of motion unlike the human body where they have different size and motion characteristics. It would be possible to modify the size of the lower vertebrae in the dummy in order to imitate the human ones and change the intervertebral rubbers between each one to replicate the motion pattern.

Tension and compression forces were not considered in the prototype and they should be taken into account to improve the biofidelity of the neck. A system to replicate them could be added to the model. An idea would be to allow possible displacements between vertebrae by means of changing the attachment design. The circular hole, where the lower pin is placed, could be increased or changed its shape (from circular to ellipsoid for example) in order to place a material between the walls of the hole and the pin itself. A rubber material with the right stiffness properties would allow the vertebrae to have a relative displacement to the adjacent vertebra being able to replicate the compression, tension and shear properties that human neck has.

Finally, durability and repeatability must be studied on the dummy. Several tests run under the same conditions are recommended to compare the parameters of interest from test to test and to check the durability of the different components of the prototype. A thorough analysis of the rubber cushions repeatability should be made. It is important to find out the required amount of time for each piece of rubber to recover its initial state, before the tests are capable to be repeated with the same the polymer responses.

# REFERENCES

1. Ashby, M.F. (1999) *Materials Selection in Mechanical Design 2nd Edition*, Butterworth Heinemann ISBN 0-7506-4357-9, England.

2. Camacho, D.L., Nightingale R.W., Robinette J.J., Vanguri, S.K., Coates, D.J. and Myers, B.S. Experimental flexibility measurements for the development of a computational head-neck model validated for near-vertex head impact. *In Proceedings of the 41st Stapp Car Crash Conference*, pages 473–486. Society of Automotive Engineers, 1997. SAE paper No. 973345.

3. Cappon, H., Philippens, M., van Ratingen, M., Wismans, J., Svensson, M., Schmitt, K.-U. (2003) Reduction of Whiplash Injury in other Modes than Rear-end Impact. *Proc. Int. Whiplash Trauma Congr.*, Oct 9-10, 2003, Denver, CO USA.

4. Carlsson, C. (2001) *An Omni Directional Dummy Neck Prototype Reproducing the Intervertebral Motion Constrains in Detail.* Master Thesis, Chalmers University of Technology, Göteborg, Sweden.

5. Carola, R., Harley, J.P., Noback, C.P.(1994) *Human Anatomy&Physiology* International Edition.

6. Condoor, S.S. (2002) *Mechanical Design Modelling using ProEngineering* McGraw-Hill, USA.

7. Davidson, J. (1999) *BioRID II Final Report* Crash Safety Division, Chalmers University of Technology, Göteborg, Sweden.

8. De Jager, M.K.J. (1996) *Mathematical Head-Neck Models for Acceleration Impacts.* PhD thesis, University of Eindhoven, Holland.

9. Feipel, V., Rondelet, B., Le Pallec, JP., Rooze, M. Normal global motion of the cervical spine: an electrogoniometric study. *Clinical Biomechanics 14*, pp 462-470, 1999.

10. Friedman, D., Friedman, K. (1993) Frontal offset and angled impact passive protection, *SAE paper No. 930637*.

11. Gent, A.N. (2001) *Engineering with Rubber. How to design rubber components.* 2nd Edition, Hanser Gardner ISBN 3-446-21403-8 Germany.

12. Goel, V.K., Clark, C.R., McGowan, D. and Goyal, S. An in-vitro study of the kinematics of the normal, injured and stabilized cervical spine. *Journal of Biomechanics 17*, pp 363-376, 1984.

13. Goel, V.K., Clark, C.R., Harris, K.G. and Schulte, K.R. Kinematics of the cervical spine: effects of multiple total laminectomy and facet wiring. *Journal of Orthopaedic Research 6*, pp 611-619, 1988.

14. Goel, V.K., Clark, C.R., Gallaes, K. and Liu, Y.K. Moment-rotation relationships of the ligamentous occipito-atlanto-axial complex. *Journal of Biomechanics 21*, pp 673-680, 1988.

15. Hell, W.; Langwieder, K.; W., Walz, F. Occurrence of reported cervical spine injuries in car accidents and improved safety standards for rear-end impacts. *WAD-conference*, Vancouver, 1999.

16. Hertz, D.J.Jr and Farinella, A.C. (1998) *Shore A Durometer and Engineering*. Seals Eastern Technical Publications Online, USA.

17. Huelke, D.F., Moffart, E.A., Mendelsohn, R.A., Melvin,J.W. (1979) Anatomy of the Human Cervical Spine and Associated Structures. *SAE Congress and Exposition*, Cobo Hall, Detroit, USA.

18. Kapandji, I.A. (1974) *The Physiology of the Joints*. Churchill Livingstone, Edinburgh, UK.

19. Linder, A. (2001) *Neck Injuries in Rear Impacts: Dummy Neck Development: Dummy Evaluation and Test Condition Specifications.* Ph.D.Thesis Chalmers University of Technology, Göteborg, ISSN 0346-718X Sweden.

20. LoPresti, E., Brienza D.M., Angelo J., Gilbertson L., Sakai J. (2000) *Neck Range of Motion and Use of Computer Head Controls* University of Pittsburgh, USA

21. Lövsund, P., Å. Nygren, B. Salen, and C. Tingvall. Neck injuries in rear end collisions among front and rear seat occupants. *In International Conference on the Biomechanics of Impacts*, pp.319-325. IRCOBI, 1988.

22. Mannion, A.F., Klein, G.N., Dvorak, J., Lanz, C. Range of global motion of the cervical spine: intraindividual reliability and the influence of measurement device *Eur Spine J  9* pp 379–385, 2000.

23. Moroney, S.P., Schultz, A.B., Miller, J.A.A. and Andersson, G.B.J. Load-displacement properties of lower cervical spine motion segments. *Journal of Biomechanics 21*, pp 769-779, 1988.

24. Oda, T., Panjabi, M.M., Crisco III, J.J., Bueff, H.U., Grob, D. and Dvorak, J. Role of tectorial membrane in the stability of the upper cervical spine. *Clinical Biomechanics 7*, pp 201-207, 1992.

25. Panjabi, M.M., Summers, D.J., Pelker, R.R., Videman, T., Friedlaender, G.E. and Southwick, W.O. Three-dimensional load-displacement  curves due to forces on the cervical spine. *Journal of Orthopaedic Research 4*, pp 152-161, 1986.

26. Panjabi, M.M., Lydon, C., Vasavada, A., Grob, D, Crisco III, J.J. and Dvorak, J. On the understanding of clinical instability. *Spine 19*, pp 2642-2650, 1994.

27. Rivin, E.I.(1999) *Stiffness and Damping in Mechanical Design*. Marcel Dekker, Inc. ISBN  0- 8247-1722-8 USA.

28. Rizza, R. (2002) *Getting started with Pro/Engineering* Upper Saddle River, Prentice Hall, USA.

29. Seemann, M.R., Muzzy, W.H. and Lustick, L.S. Comparison of human and Hybrid III head and neck dynamic response. *In Proceedings of the 30th Stapp Car Crash Conference*. pp. 291-312. SAE, 1986. SAE Paper No. 861892.

30. Svensson, M. et al. (2002) European Enhanced Vehicle-safety Committee (EEVC) *Working Group 12 Report*, Document N°157 - Ad-Hoc Group on Whiplash Injuries.

31. White, A.A., Panjabi, M.M. (1978) *Clinical Biomechanics of the Spine*. Lippincott, USA.

32. White, A.A. and Panjabi, M.M. Clinical Biomechanics of the spine. J.B. Lippincott Company, 2$^{nd}$ edition, 1990.

33. Panjabi, M.M., Dvorak, J., Duranceau, J., Yamamoto, I., Gerber, M., Rauschning, W. and Bueff, H.U. Three-dimensional movements of the upper cervical spine. *Spine 13*, pp 726-730, 1988.

34. Panjabi, M.M., Dvorak, J., Crisco III, J.J., Oda, T., Wang, P. and Grob, D. Effects alar ligament transaction on upper cervical spine rotation. *Journal of Orthopaedic Research 9*, pp 584-593, 1991.

35. Panjabi, M.M., Dvorak, J., Crisco III, J.J., Oda, T., Hilibrand, A. and Grob, D. Flexion, extension, and lateral bending of the upper cervical spine in response to alar ligament transactions. *Journal of Spinal Disorders 4*, pp 157-167, 1991.